EXPLORATION GEOPHYSICS

The determination of the constant phase of seismic wavelet using automatic seismic well tying

Journal:	*Exploration Geophysics*
Manuscript ID	EG17161.R2
Manuscript Type:	Research Paper
Date Submitted by the Author:	12-Jul-2018
Complete List of Authors:	Wu, Hao; University of Alabama, Geological Sciences zhang, bo ; University of Alabama, the Department of Geological Sciences Cao, Danping; China University of Petroleum (East China), School of Geoscience
Keyword:	Phase, Wavelet

SCHOLARONE™
Manuscripts

The determination of the constant phase of seismic wavelet using automatic seismic well tying

Hao Wu[1], Bo Zhang[1], and Danping Cao[2]

[1]The University of Alabama, Department of Geological Science

[2]China University of Petroleum (East China), School of Geoscience

hwu43@crimson.ua.edu, bzhang33@ua.edu, and caodp@upc.edu.cn

Corresponding author:

Bo Zhang

The University of Alabama, Department of Geological Science

bzhang33@ua.edu

ABSTRACT

Seismic wavelet estimation is the bed rock for the seismic well tying and seismic inversion but remains a challenging task. Huge efforts have spent on seismic wavelet estimation and determining amplitude and phase spectrum is a time consuming task. In this paper, we develop a workflow to determine the constant phase of estimated wavelet automatically. Our workflow begins with statistical wavelet estimation and seismic well tie. We then extract a new seismic wavelet with constant phase by using the well and seismic data together. To obtain the best phase for the extracted wavelet using well and seismic data, we rotate the phase of the wavelet according to a user-defined increment and perform automatic seismic well tying for each phase-rotated wavelet. The phase, which reaches the maximum correlation coefficient between synthetic and seismic data, is regarded as the best phase for wavelets in each iteration. We next update the time-depth relation according to the result of best seismic well tie (the maximum correlation coefficient). We repeat the wavelet estimation using well and seismic data, phase rotation, automatic seismic well tie, and time-depth updating procedures until the difference of wavelets, and time-depth relationships in the current and previous iteration is smaller than a user-defined threshold.

Keyword: **Seismic well tie**, **Wavelet**, **Phase**, **DTW**

INTRODUCTION

Seismic wavelet estimation is one of the key procedures for seismic interpretation and inversion. The determination of a seismic wavelet includes amplitude and phase spectrum estimation. Wavelet estimation methods can be classified into three main categories: (1) directly deterministic measuring the wavelet, (2) statistically extracting the wavelet from the seismic data and (3) extracting the wavelet by using well-log and seismic data. The deterministic methods require that a seismic-well tie already exists, while the statistical method extracts an average wavelet from a specified window of 3D seismic data (Edgar and van der Baan, 2011). Wavelet estimation using well and seismic data incorporates the "prior" reflectivity information in the wavelet estimation (Richard et al., 1988). Statistical wavelets can be estimated from only the seismic data without appealing to well logs. Most of the statistical wavelet estimations are based on the assumption that seismic traces are a convolution of the earth's reflectivity and a temporally and spatially invariant zero or minimum phase wavelet. Statistical wavelets assume that the autocorrelations of amplitude spectra of the seismic data are approximately equal to the seismic wavelet (Yilmaz, 2001).

The determination of the phase spectrum of a seismic wavelet is as important as the determination of the amplitude spectrum of a seismic wavelet. Van der Baan (2008) illustrated that the phase mismatch might result in incorrect horizon picking or seismic well tying. Many techniques have been developed to identify the phase seismic wavelet phase spectrum. Compared to the amplitude spectrum estimation of seismic wavelets, determining the phase spectrum is far more difficult and significantly affects seismic inversions (Hampson, 2007). Wiggins (1978) estimated the phase of seismic wavelet through the minimum entropy deconvolution. This technique does not need to assume the phase characteristics of a seismic

wavelet. White (1988) proposed to estimate the phase of a seismic wavelet by integrating the maximum kurtosis theory. The advantage of White's method is that there is no requirement for a Gaussian distribution of the subsurface reflectivity series. Levy and Oldenburg (1987) present a method that uses the varimax norm to estimate the residual phase directly; it can make the phase correction automatically. Van der Baan (2008) developed a method, which is based on the maximum kurtosis estimation to obtain time-varying wavelets. It is robust enough to detect time-varying phase change.

Hampson (2007) pointed out that a constant phase wavelet estimation using well is the most robust method. The estimation of amplitude and phase spectrum of wavelet using seismic does not consider the "prior" reflectivity information contained in the well logs (Richard et al., 1988). There are two main steps for the wavelets estimation using seismic and well data. The first step includes amplitude spectrum estimation using seismic data and reflectivity computed using well logs. The second step is to obtain the optimum phase of the wavelet through seismic-well tying. Nyman (1987) proposed an interactive methodology for the estimation of a seismic wavelet using well control. Their method separately estimated the wavelet's amplitude and phase spectrum. The amplitude spectrum estimation is simply averaging of the ratio between seismic traces spectrum and reflectivity spectrum. Nyman (1987) assumed a constant phase spectrum, and obtained it through phase and time shifting which maximized the correlation with the synthetic and seismic traces. To obtain the optimal phase for wavelet and time shift for seismic well tie, we usually need more than 10 times manual the seismic well tie and phase scanning of the seismic wavelet, which is therefore time-consuming. Richard et al. (1988) estimated a linear phase wavelet using well-control. In this paper, we propose a workflow to expedite the estimation of constant phase of seismic wavelet in the seismic well tying. Our workflow is

similar with the workflow that proposed by Hampson (2007). However, our workflow can heavily expedite the process of phase determination. We substitute the process of manually optimum phase determination using an automatic procedure. We first perform the scanning of phase rotation of the wavelet according to the user-defined range and increment step. We then automatically obtain the corresponding time shift, synthetic squeezing and stretching for each candidate phase by using dynamic time warping (DTW) (Sakoe and Chiba, 1978). The phase that yields the largest correlation coefficient between seismic and synthetic is considered as the best phase in the current loop of seismic well tie. We next estimate the amplitude spectrum of a wavelet using the new time-depth relationship. We next scan the phase and automatically perform the seismic well ties for each phase rotated wavelets. We repeat the procedure of amplitude spectrum estimation using well-log data, phase scanning, and automatic seismic well ties until we converge on a solution.

METHODOLOGY

A stacked seismic trace can be regarded as the convolution of the seismic wavelet with reflectivity series and added noise:

$$x = r * w + n \tag{1}$$

where x is the seismic trace, r is the reflectivity series, w is the wavelet, n is the noise, and $*$ denote the convolution operator. A wavelet usually is considered a transient signal. It has a start time and an end time, and its energy is confined between these two-time positions (Yilmaz, 2001).

The seismic well tie is the procedure of matching the synthetic seismogram computed using well logs and wavelet to a real seismic trace nearby the borehole place (Walden and White, 1984). We compute the reflectivity series from a velocity log, $v(z)$, and a density log, $\rho(z)$. The

synthetic seismogram is generated by convolving the reflectivity series with a user defined wavelet or a wavelet estimated from the seismic trace. In this paper, we employ DTW to perform the seismic-well tie through automatically time shifting, stretching and squeezing the synthetic seismogram. DTW is an algorithm for measuring the similarity between two signals (Muller, 2007). The objective of this algorithm is to make an alignment of the two signals through time shifting, squeezing, and stretching one of the signals.

Several researchers (Munoz and Hale, 2012. Roberto et al, 2012) have proposed to use DTW for automatic seismic well ties. Roberto et al (2014) adds a global distance constraint to DTW to prevent the nonphysical alignment. Wu and Gaumon (2017) employed DTW to perform multiple seismic well tie on the flattened syntethic and seismic traces. Error function computation is the first step for DTW to align two signal. We first apply 10 times finer sampling for the synthetic and real seismic traces. The finer interpolation of synthetic and real seismic traces realizes the similar smaller time shift strain of synthetics proposed by Hale(2013). We then use the Euclidean distance between synthetic $\mathbf{X} = (x_1, x_2, ..., x_N)$ and real seismic trace $\mathbf{Y} = (y_1, y_2, ..., y_M)$ compute the error matrix $d(i, j)$

$$d(i, j) = \sqrt{(x_i - y_j)^2} , \tag{2}$$

where $i,\ j$ is the sample index of the refined seismic and synthetic trace, respectively. The total number of samples of the seismic and synthetic traces are M and N, respectively. The second step is to step-wisely compute the accumulated error matrix $D(i, j)$ using the error matrix.

$$\begin{aligned} D(i, j) = d(i, j) + \\ \min\{D(i-1, j-1), D(i-1, j) + d(i-2, j-1), D(i, j-1) + d(i-1, j-2)\} \end{aligned} . \tag{3}$$

The final step of DTW is backtracking the minimum cost path within the accumulated error matrix

$$p_L = \arg\min\{D(M,1) \quad \dots \quad D(M,N)\} \tag{4a}$$

$$p_{l-1} = \arg\min\{D(i-1,j-1), D(i-1,j)+D(i-2,j-1), D(i,j-1)+D(i-1,j-2)\}, \tag{4b}$$

where L is the total sample number of the backtracked path. We apply the algorithm of dynamic programming to backtrack the path of minimum accumulate Euclidean distance to obtain a sequence of corresponding index pairs $p = (i,j)$, which is the best matching between the synthetic and real seismic trace.

Finally, we can shift, stretch, and squeeze the synthetic to tie it to the real seismic trace according to the tracked minimum cost path. Unfortunately, the occurrence of nonphysical alignment is unavoidable. In other words, DTW does not consider the shifting, stretching, and squeezing amount for near-by sample of a signal when aligned with another signal. Figure 1a illustrates an example of seismic (black curve) well (red curve) tie using DTW. The red arrows indicate the locations where we need severe stretching of synthetic trace to tie the seismic trace. The black arrow indicate the location where we need severe squeezing of synthetic trace to tie the seismic trace. Several methods have been proposed to address this problem. Roberto et al (2012) add a global constraint to the DTW to limit the maximum amount of permitted stretching and squeezing. Hale (2013) refine the error matrix to apply smaller shift strain and achieve smoother path slope. To avoid the severe stretching and squeezing in the real world of seismic well tie, we add a weight term to the accumulated error matrix

$$
\begin{aligned}
w_{l1} &= \lambda\frac{(t_{l+1}-t_l)-(t_l-t_{l-1})}{(\tau_{l+1}-\tau_l)-(\tau_l-\tau_{l-1})} = \lambda\frac{1-(t_l-t_{l-1})}{1-(\tau_l-\tau_{l-1})}\\
w_{l2} &= \lambda\frac{(t_{l+1}-t_l)-(t_l-t_{l-1})}{(\tau_{l+1}-\tau_l)-(\tau_l-\tau_{l-1})} = \lambda\frac{1-(t_l-t_{l-1})}{2-(\tau_l-\tau_{l-1})}\\
w_{l3} &= \lambda\frac{(t_{l+1}-t_l)-(t_l-t_{l-1})}{(\tau_{l+1}-\tau_l)-(\tau_l-\tau_{l-1})} = \lambda\frac{2-(t_l-t_{l-1})}{1-(\tau_l-\tau_{l-1})}
\end{aligned}
\tag{5a}
$$

$$p_l = argmin[D(i-1,j-1)+w_{l1}, D(i-1,j)+D(i-2,j-1)+w_{l2}, D(i,j-1)+D(i-1,j-2)+w_{l3}] \tag{5b}$$

where the λ denotes the user defined weight, (t_l, τ_l) denote the position index of the optimal matching path. Our proposed weight terms are the second derivative of the unwrapped path. We are expected to avoid the abrupt change of unwrapped path by minimizing our weighted term. The abrupt change of the path corresponds to severe stretching or squeezing of the synthetic in the seismic well tying, which can limit the variation of path slope between last step and current step. The white curve in Figure 1b shows the tracked optimum cost path using equation 5. We successfully avoid the severe stretching and squeezing shown in Figure 1a. Figures 2a and 2b shows the seismic well tie using the unweighted and weighted backtracking methods, respectively. The cross-correlation coefficients in Figure 2a and 2b are 0.652 and 0.801, respectively.

Figure 3 shows the proposed workflow used to determine the phase of wavelet using the improved DTW. We obtain the amplitude spectrum of proper wavelet using and seismic data and the constant phase by comparing the automatic seismic-well tie for each candidate phase. The workflow is an iterative procedure. It begins with an automatic seismic well tie by DTW. The reflectivity is computed from the well log, and the initial wavelet is the statistical wavelet that is computed from the whole seismic trace. The next step is to extract the wavelet using well and seismic data (Hampson, 2007). We then rotate the phase of the input wavelet and convolve with the reflectivity to compute a set of synthetic seismogram. We next apply DTW to make an alignment between seismic trace and synthetic seismograms and calculate the correlation between the synthetic and seismic trace. We choose the phase which has the maximum correlation coefficients as the best phase and update the time-depth relationship of the well log. We repeat the steps of extracting wavelet using well and seismic data, phase rotation and seismic well tie, phase selecting and   time-depth relationship updating until and the wavelets and time-

depth relationships in current and previous iteration are smaller than a user-defined threshold (equation 6).

$$\frac{\sum_i \left| W^{(k+1)}(f_i) - W^{(k)}(f_i) \right|}{\sum_i W^{(k)}(f_i)} < 0.001 \tag{6a}$$

$$\left| \varphi^{(k+1)} - \varphi^{(k)} \right| < 2 \tag{6b}$$

$$\frac{\sum \left| T^{(k+1)}(j) - T^{(k)}(j) \right|}{N} < 0.001 \tag{6c}$$

where $W^{(k)}(f_i)$ is the amplitude spectrum of the wavelet in the kth iteration of seismic well tie,

φ is the constant phase of the wavelet, $T_k(i)$ is the time shift for the jth sample of the synthetic,

and N is the total sample number of the synthetic.

APPLICATION

Real data example

To demonstrate the effectiveness of our workflow, we apply it to a seismic survey acquired over the Fort Worth Basin. We use one well within the seismic survey to demonstrate the proposed workflow. Figure 4 shows the extracted 200 ms statistical wavelet from the poststack seismic using the Hampson-Russell commercial software. The extracted statistical wavelet is used as the initial wavelet for the seismic well tie using DTW. The first, second, third, and fourth panels in Figure 5 are the density, P-wave velocity, computed reflectivity, and computed synthetic, respectively. We compute the synthetic through the convolution between the reflectivity shown in the third panel of Figure 5 and wavelet shown in Figure 4. Figure 6a shows the synthetic (red curve) overlaid on the real seismic trace at the wellbore location before automatic seismic well tie. The horizontal axis is the sample index of the two sequences

(synthetic and real seismic trace). In our case, we only have p-wave and density logs within a limited depth zone. The length of the synthetic is much smaller than that of the seismic traces. Figure 6b shows the results of automatic seismic-well tie using the statistical wavelet.

We begin our phase determination after we obtain a rough seismic well tie shown in Figure 6b. We iteratively extract the wavelet using well and seismic data with constant phase. Figure 7 shows the extracted wavelet using well and seismic data in the first iteration. The initial phase of the exacted wavelet shown in Figure 7 is 129°. We then rotate the phase of the wavelet and convolve the phase rotated wavelet with the reflectivity to generate the synthetic seismogram. In this paper, we rotated the phase from 0° to 359° with a step of 1°. Figure 8 shows six representative phase rotated wavelets with rotation amount of 0, 60°, 120°, 180°, 240°, 300°. The phase of the rotated wavelets shown in Figure 8 are 129°, 189°, 249°, 309°, 9°, 69°, respectively. We next apply DTW to perform the automatic seismic well tie between the synthetic and seismic trace and compute the correlation coefficient for each seismic well tie. Figure 9 shows six representative results of automatic seismic well ties in the first iteration for the 0, 60°, 120°, 180°, 240°, 300° phase rotated wavelets. We automatically perform seismic well ties 360 times for each iteration and roughly need 30 seconds in each iteration. Figure 10 shows the cross-correlation coefficient varying with phases of wavelets. We obtain the cross-correlation coefficients in Figure 10 by comparing the similarity between synthetic and seismic trace after the seismic well ties. According to the cross-correlation coefficients shown in Figure 10, the best phase for the wavelet in the first iteration is 125°. The last processing in each iteration is updating the time-depth relationship according to the seismic well tie with the maximum correlation coefficient.

There are negligible changes for both wavelets and seismic well ties after 15 iterations in our case. Figure 11 shows the seismic well tie for each iteration. The red and black curve are the synthetic and seismic traces, respectively. Note the changes of the seismic well tie is negligible starting from 8th iteration. Figure 12 shows the accumulated error matrix and optimal warping minimum cost path (white curve). Figure 13 shows wavelets changing with the iteration number of seismic well tie. The black and red curve are the wavelet with best phase in each iteration and the final optimum wavelet, respectively. Note that there are negligible changes for the shape and phase of the seismic wavelet after 15 times iteration. We obtain our best wavelet after 15 times in our application according to the criteria defined in Equation 6.

Comparison with conventional DTW

To illustrate the robustness of our proposed workflow, we also compare our method with the conventional DTW. We selected the same seismic data and well log data from the Fort Worth Basin. We iteratively apply DTW and our method to align the synthetic seismogram from the well log with the real seismic trace. The black and red curves in the first panel of Figure 14-15 are the real seismic trace and original synthetic seismogram, respectively. The black and red curves in the second, third and fourth panel of Figure 14-15 are the 1st to 3rd iteration result of real seismic trace and tied synthetic seismogram by DTW and our method, respectively. In figure 14, the synthetic seismogram shows some abrupt velocity changing part and based on the well top data, the synthetic tied to the wrong position of the seismic trace. Noted that in Figure 15, using our method get higher cross-correlation, the synthetic has tied to the right position of seismic trace and the change of time-depth relationship has meet the defined threshold.

CONCLUSIONS

We present a novel workflow to estimate the wavelet phase automatically. In this paper, we first improve the DTW algorithm by adding a second derivative weight in the error matrix computation. The weighted term is designed for avoid the severe stretching or squeezing of synthetic in the process of seismic well ties. We then obtain the best phase of a wavelet by performing iteratively automatic seismic well tie using our proposed modified DTW algorithm. The application and comparison illustrate that our workflow not only obtains the best phase of wavelet for the seismic well but also improves the quality of the seismic well tie. Moreover, our workflow also heavily expedite the process of wavelet phase estimation and seismic well tie when compared to the manual seismic well tie.

LIST OF FIGURE CAPTIONS

Figure 1. Cartoon illustrating seismic well result using original and imprvoed DTW aglorihtms. (a) The accumulated error matrix and optimal warping path using original DWT. (b) The accumulated error matrix and optimal warping path using improved DTW.

Figure 2. The seismic well tie results using (a) DTW and (b) improved DTW. The improved DTW successfully avoids the severe stretching and squeezing.

Figure 3. The proposed workflow of the seismic phase determination.

Figure 4. The initial extracted statistical wavelet using commercial software.

Figure 5. The well logs and synthetic used for seismic well tie. The first, second, third, and fourth panel are the density log, velocity log, computed reflectivity and computed synthetic seismogram, respectively.

Figure 6. The synthetic (red) and seismic (black) (a) before and (b) after seismic well tie.

Figure 7. The extracted wavelet using well and seismic data in the first iteration.

Figure 8. The six representative phase rotated wavelets in the first iteration of seismic well tie. The initial phase of the wavelet is 129°. The phases of the phase rotated wavelets are 129°, 189°, 249°, 309°, 9°, and 69°.

Figure 9. The six representative results of automatic seismic well tie in the first iteration for the 0, 60°, 120°, 180°, 0°, and 300o phase rotated wavelets.

Figure 10. The cross-correlation coefficient between seismic well tie for the phase rotated wavelets the first iteration.

Figure 11. The seismic well tie results in each iteration.

Figure 12. The accumulated error matrix overlaid with the optimum minimum cost path (white curve) in each iteration.

Figure 13. The wavelets with the best phases in each iteration. The black and red curves are the wavelet with the best phase and the final best wavelets, respectively.

Figure 14. The test of DTW in real data. The first panel shows the original synthetic seismogram (red) overlaid on the seismic trace (black), the second to fourth panels shows the 1st to 3rd iteration results of seismic trace (black) and tied synthetic seismogram (red). The tied synthetic seismogram are tied to the wrong position and shows some abrupt changing of time-depth relationship.

Figure 15. Illustrating that our proposed method applied on the real seismic data. The first panel shows the original synthetic seismogram (red) overlaid on the seismic trace (black), the second to fourth panels shows the 1st to 3rd iteration results of seismic trace (black) and tied synthetic seismogram (red). Noted that the tied synthetic seismogram meet the defined threshold and get an excellent seismic well tie after three times iteration.

REFERENCE

Buland, A., and H. More, 2003, Jonint AVO inversion, wavelet estimation and noise-level estimation using a spatially coupled hierarchical Bayesian model, Geophysical Prospecting, **51**, 531-550.

Edgar, J., and M. van der Baan, 2011, How reliable is statistical wavelet estimation?: Geophysics, **76**, no. 4, V59–V68.

Hampson, D., 2007, Theory of the Strata program: Technical report, CGG Hampson-Russell.

Hale, D., 2013, Dynamic warping of seismic images: Geophysics, 78, no. 2, S105–S115.

Herrera, R., H., and M., van der Baan, 2012, Guided seismic-to-well tying based on dynamic time warping, SEG Expanded Abstracts

Herrera, R. H., S. Fomel, and M. van der Baan, 2014, Automatic approaches for seismic to well tying: Interpretation, **2**, no. 2, SD101–SD109

Levy, S., and D. W. Oldenburg, 1987, Automatic phase correction of common-midpoint stacked data: Geophysics, **52**, 51-59.

Liner, C. L., 2002, Phase, phase, phase: The Leading Edge, **21**, 456-457.

Longbottom, J., A. T. Walden, and R.E. White, 1988, Principles and application of maximum kurtosis phase estimation: Geophysical Prospecting, **36**, 115-138.

Mueller, M., 2007, Dynamic time warping in information retrieval for music and motion: Springer.

Muñoz, A., and D. Hale, 2012, Automatically tying well logs to seismic data, CWP-725.

Muñoz, A., and D. Hale, 2015, Automatic simultaneous multiple well ties: Geophysics, **80**, no. 5, IM45–IM51.

Nyman, D. C., M. J. Parry, and R. D. Knight, 1987, Seismic wavelet estimation using well control, SEG Expanded Abstracts, 211-213.

Richard, V., and J. Brac, 1988, Wavelet analysis using well log information. SEG Expanded Abstracts, 946-949.Robinson, E. A., 1957, Predictive decomposition of seismic traces: Geophysics, **22**,767-778.

Robinson, E. A., and S. Treitel, 1967, Principles of digital Wiener filtering: Geophysical Prospecting, **15**, 311-332.

Sakoe, H., and S. Chiba, 1978, Dynamic programming algorithm optimization for spoken word recognition: IEEE Transactions on Acoustics, Speech, and Signal Processing, **26**, 43-49.

Stone, D. G., 1984, Wavelet estimation: Proc. IEEE, **72**, 1394-1402.

van der Baan, M., 2008, Time-varying wavelet estimation and deconvolution by kurtosis maximization: Geophysics, **73**, no.2, V11-V18.

van der Baan, M., and S. Fomel, 2009, Nonstationary phase estimation using regularized local kurtosis maximization: Geophysics, 74, A75-A80.

van der Baan, M., S. Fomel, and M. Perz, 2010, Nonstationary phase estimation: A tool for seismic interpretation?: The Leading Edge, **29**, 1020-1026.

Walden, A. T., and J. W. J. Hosken, 1985, An investigation of the spectral properties of primary reflection coefficients: Geophysical Prospecting, **33**, 400-435.

Walden, A. T., and R. E. White, 1984, On errors of fit and accuracy in matching synthetic seismograms and seismic traces: Geophysical Prospecting, **32**, 871-891.

White, R. E., 1988, Maximum kurtosis phase correction: Geophysical Journal International, **95**, 371-389.

White, R. E., and P. N. S. O'Brien, 1974, Estimation of the primary seismic pulse: Geophysical Prospecting, **22**, 627-651.

White, R., and T. Hu, 1997, How accurate can a well tie be?: SEG Expanded Abstracts, **16**, 816.

White, R., and R. Simm, 2002, Phase, polarity and the interpreter's wavelet: EAGE first break, **20**, 277-281.

White, R., and R. Simm, 2003, Tutorial: Good practice in well ties: EAGE first break, **21**, 75-83.

Wiggins, R., 1978, Minimum entropy deconvolution: Geoexploration, **16**, 21-35.

Wu, X., and G. Caumon, 2016, Simultaneous multiple well-seismic ties using flattened synthetic and real seismograms: Geophysics, **82**, no. 1, IM13–IM20

Yilmaz, Ö., 2001, Seismic data analysis: processing, inversion, and interpretation of seismic data: Society of Exploration Geophysicists.

Figure 1a

Figure 1b

(a)

Figure 2a

(b)

Figure 2b

Figure 3

Figure 4

Figure 5

(a)
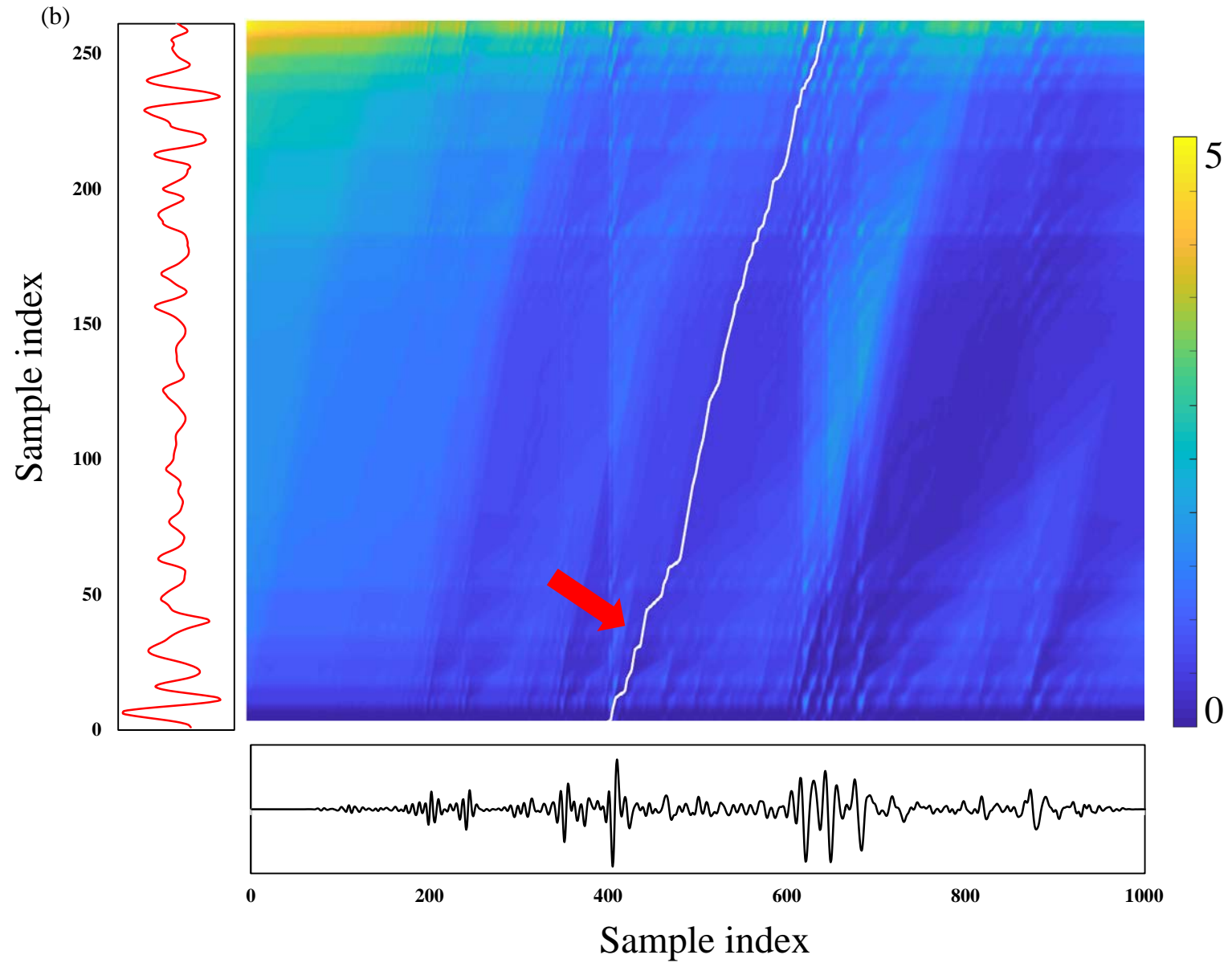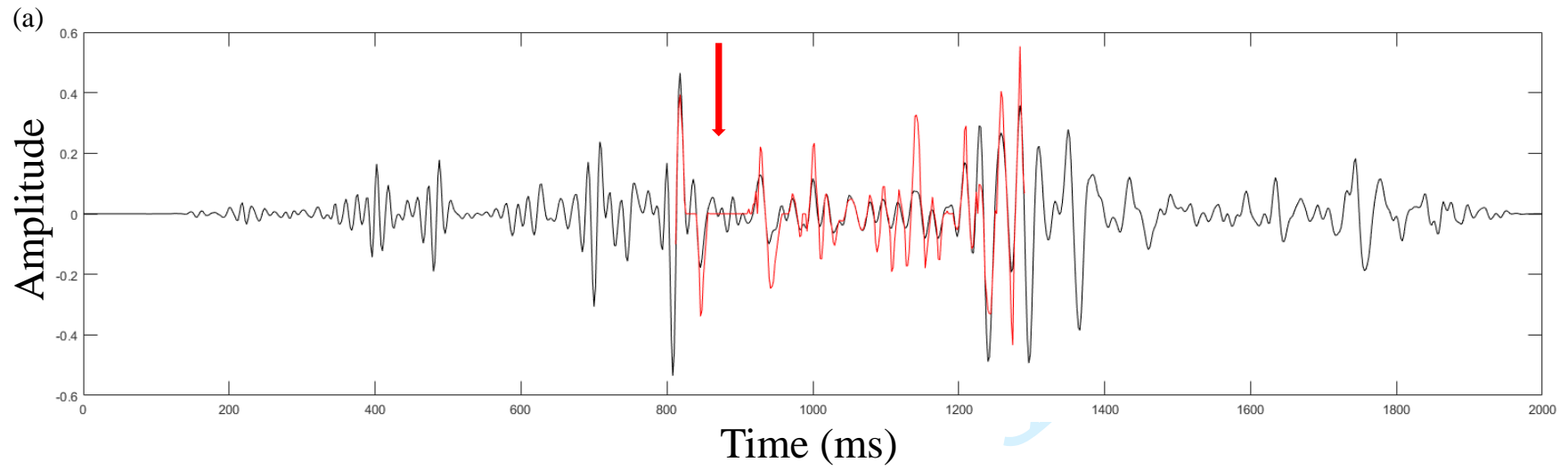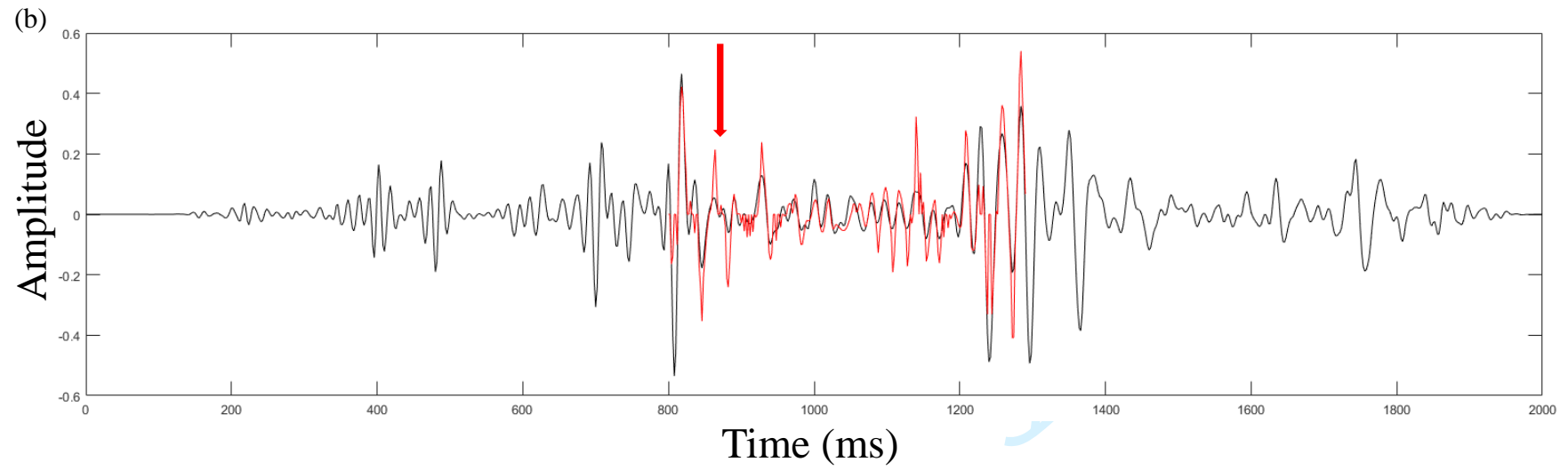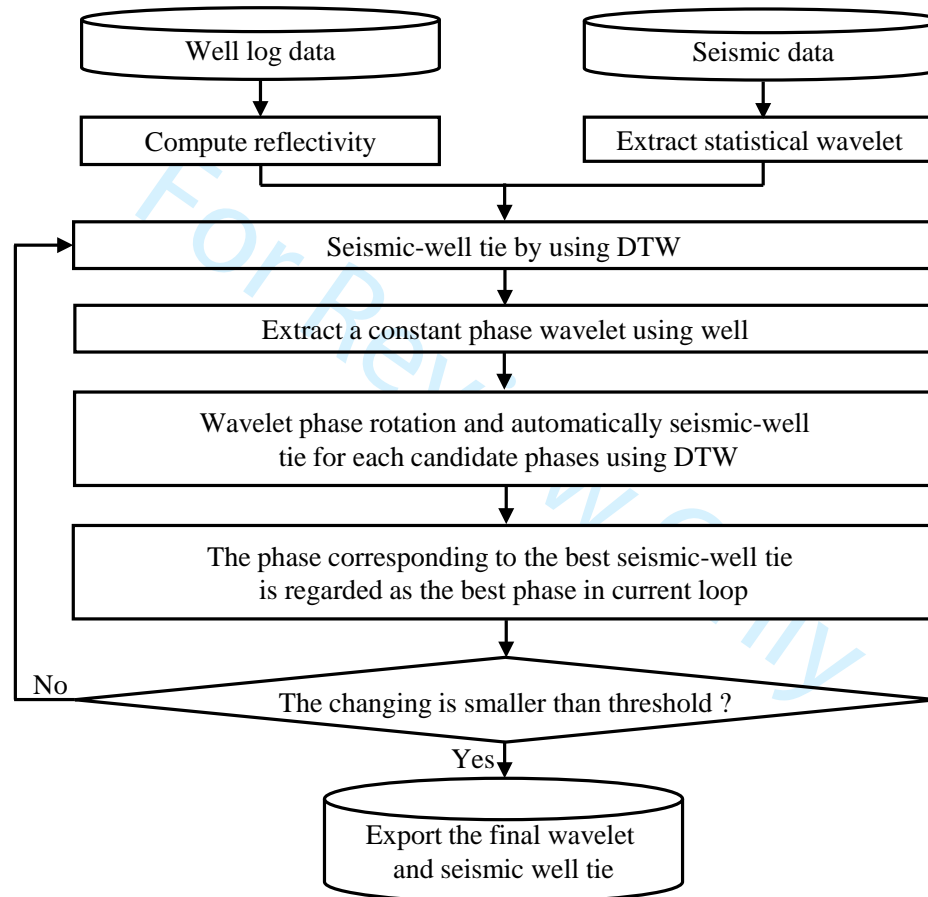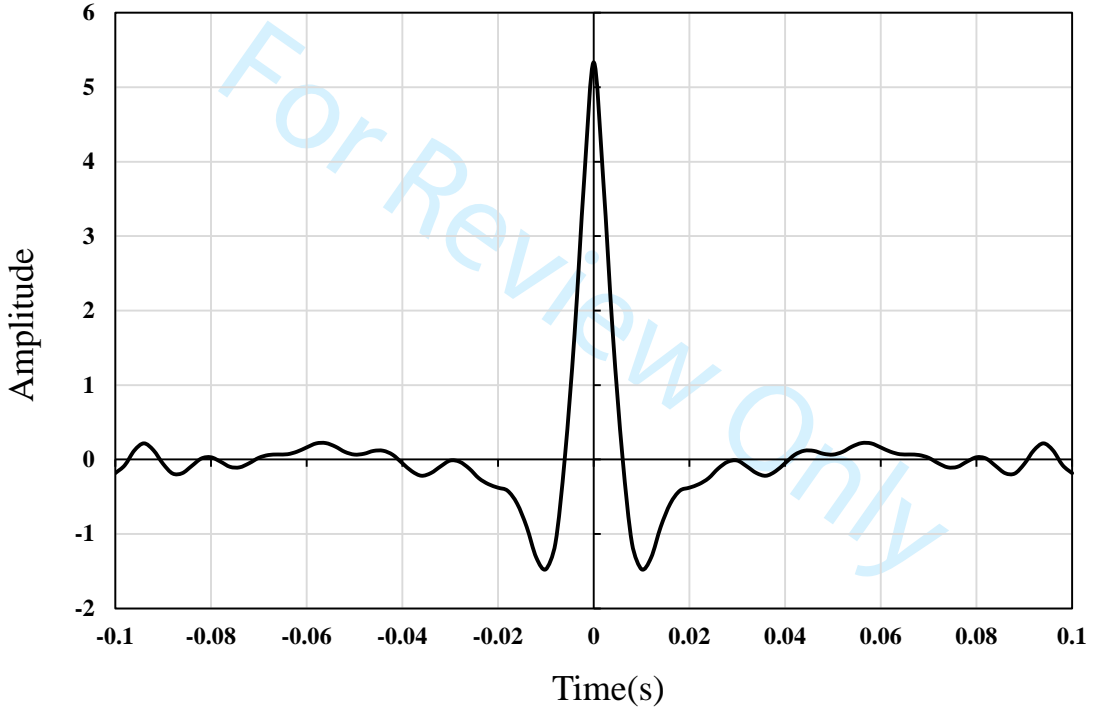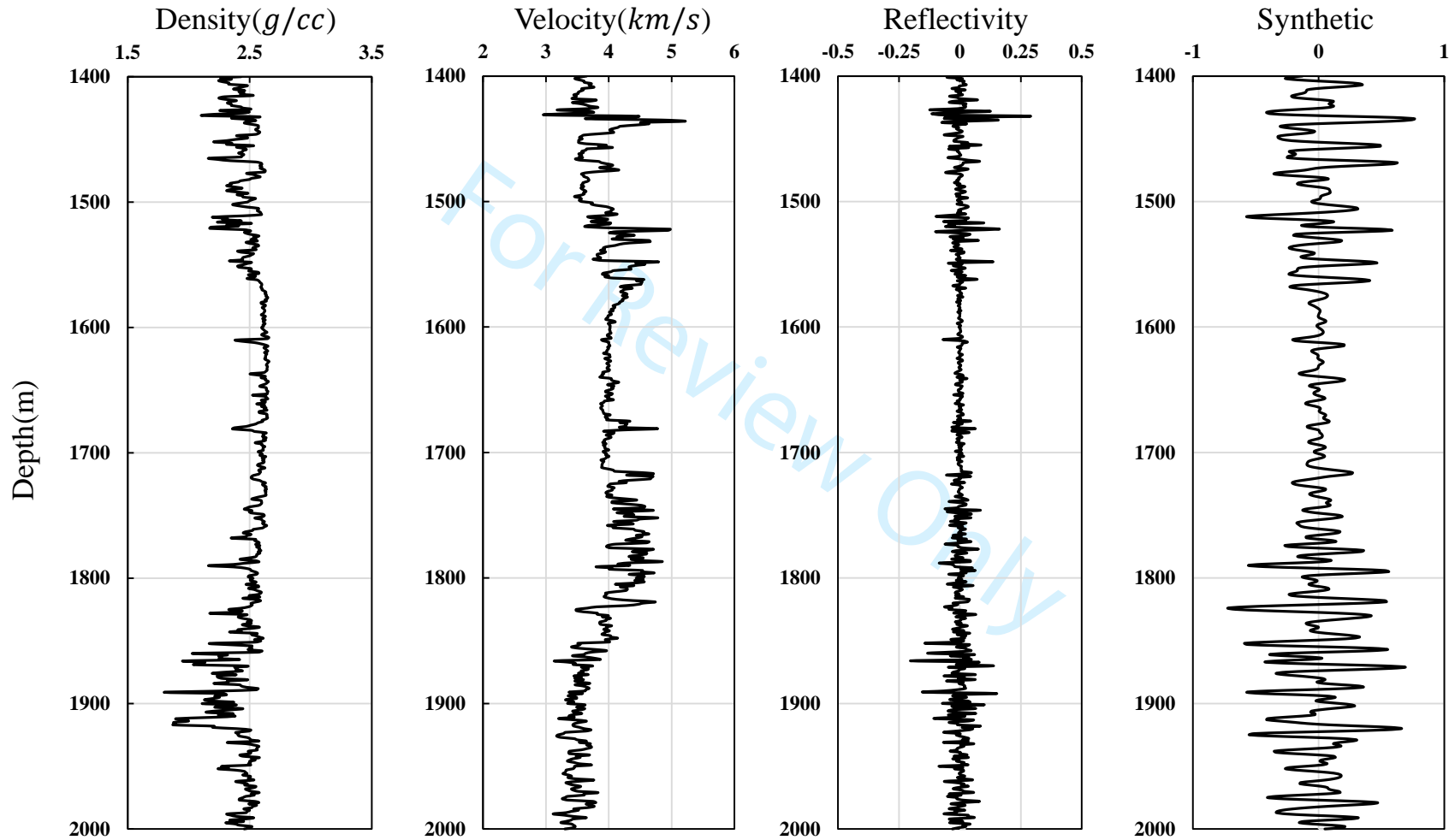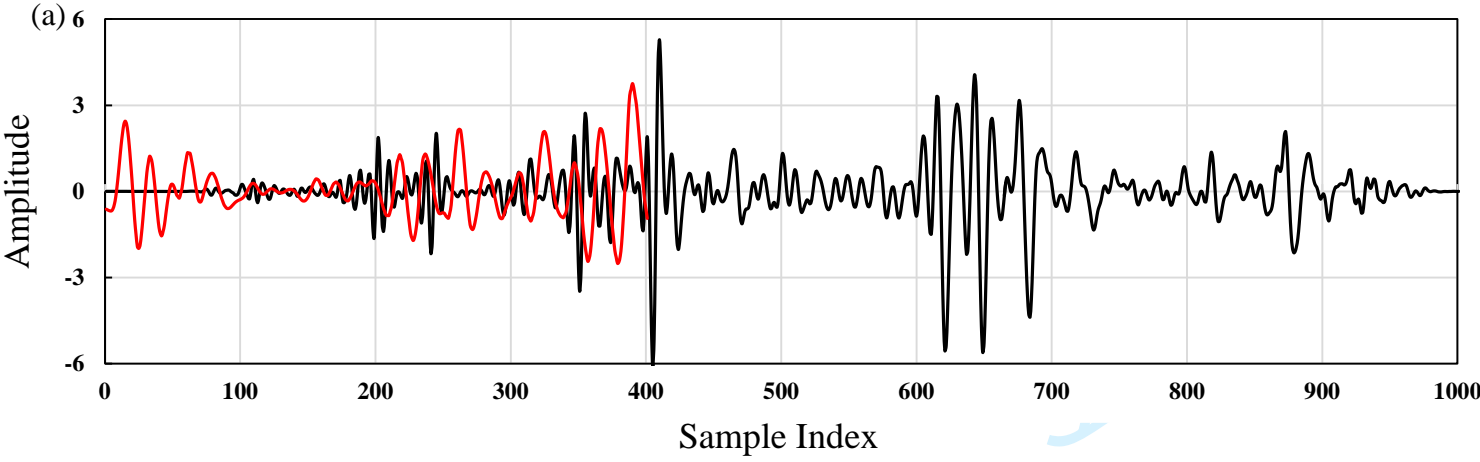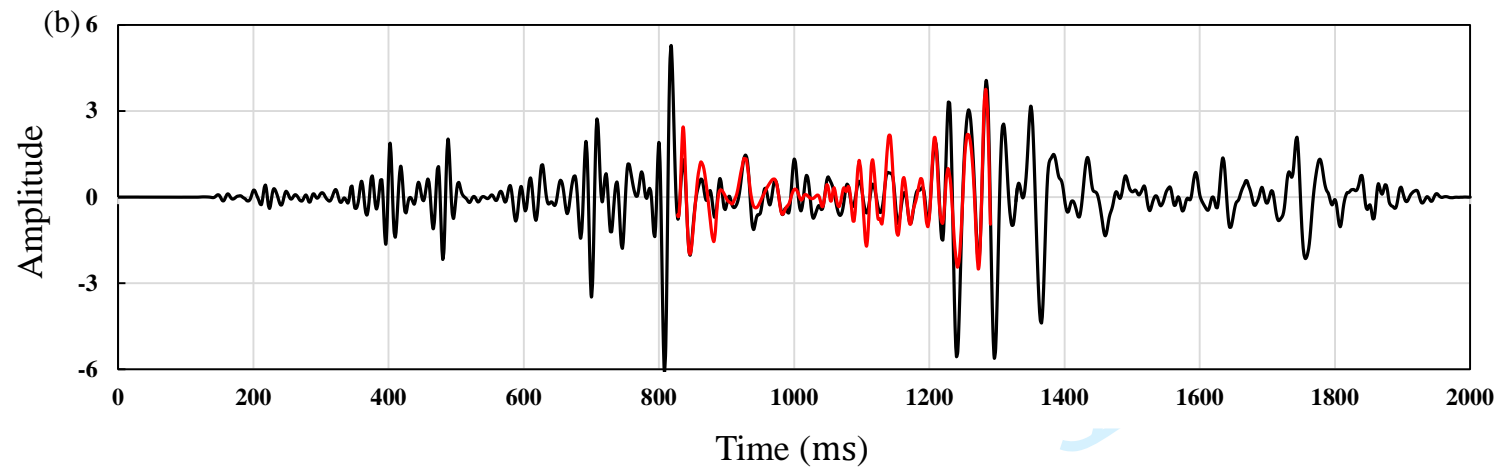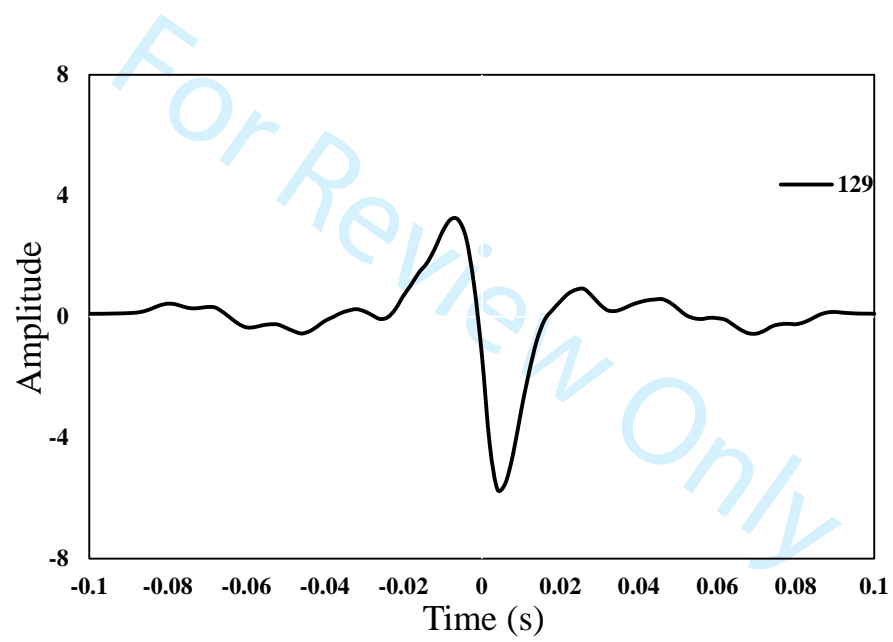
Figure 6a
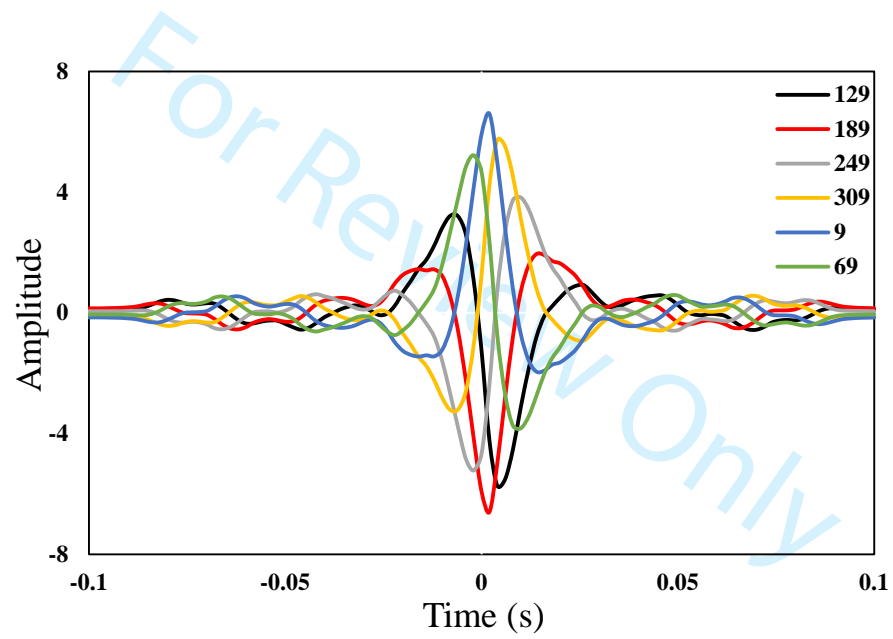
Figure 6b
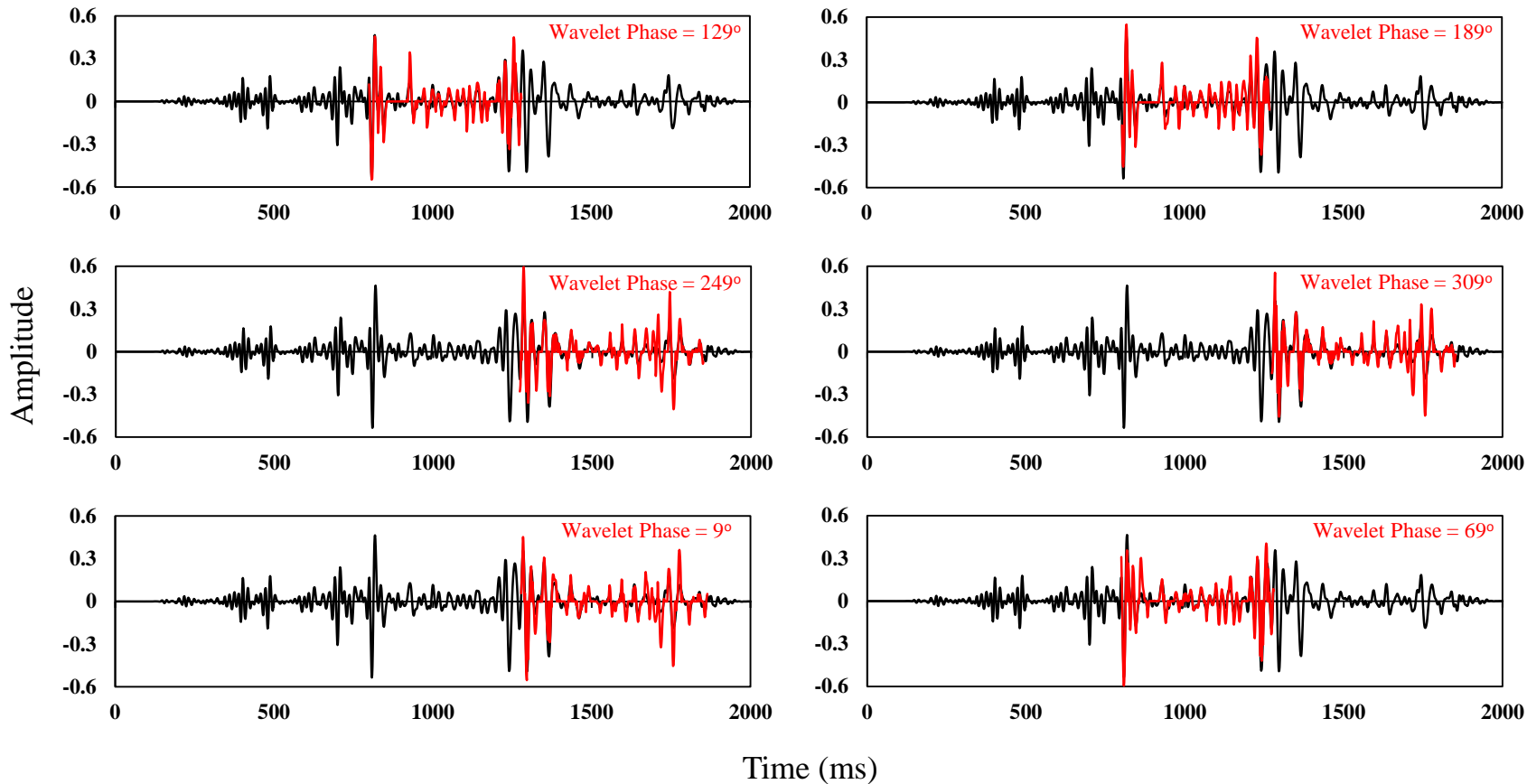
Figure 7

Figure 8

Figure 9
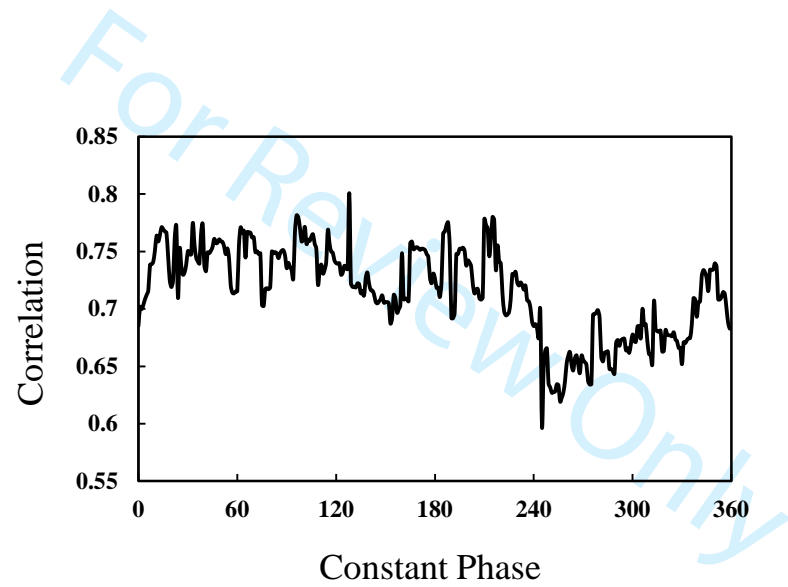
Figure 10
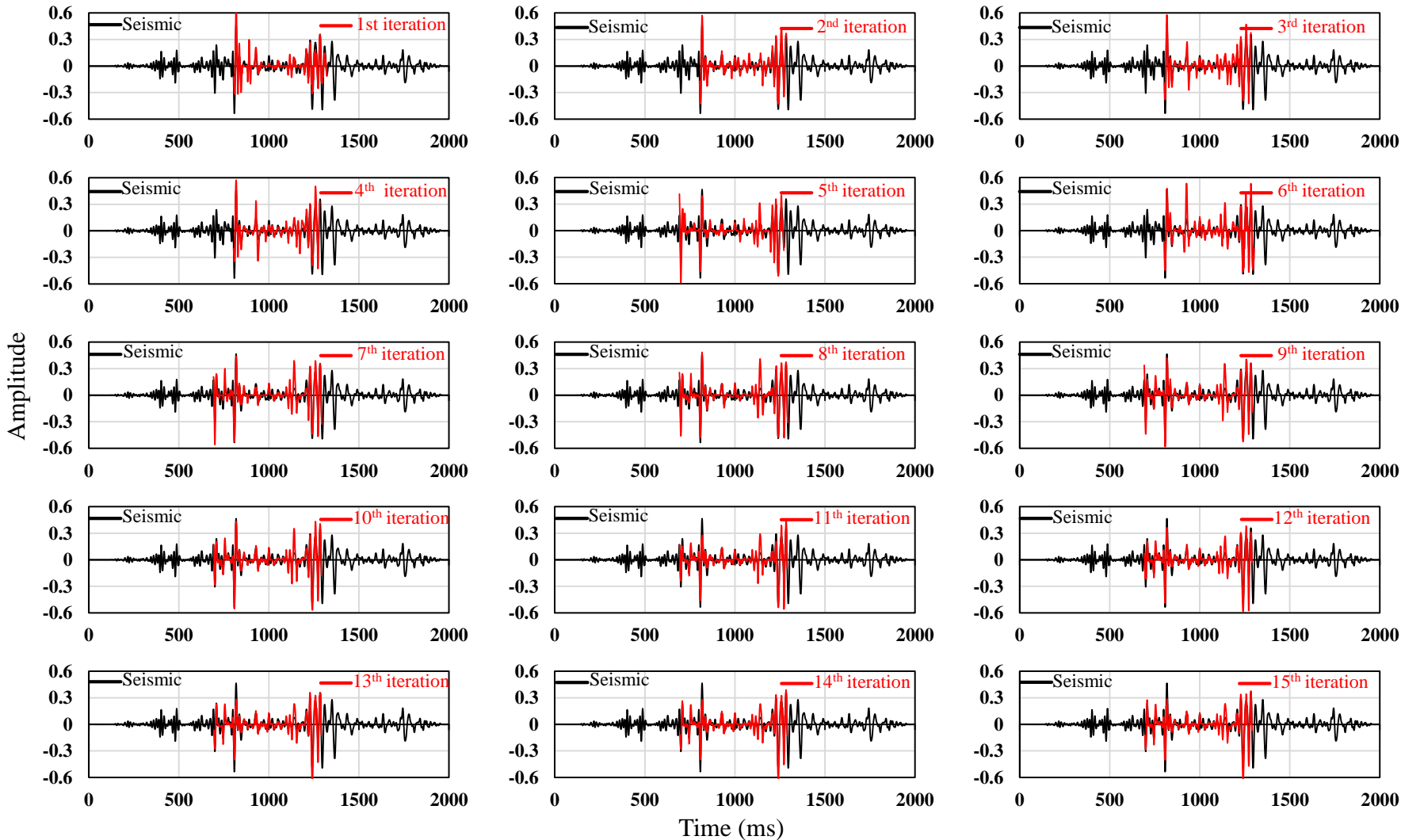
Figure 11
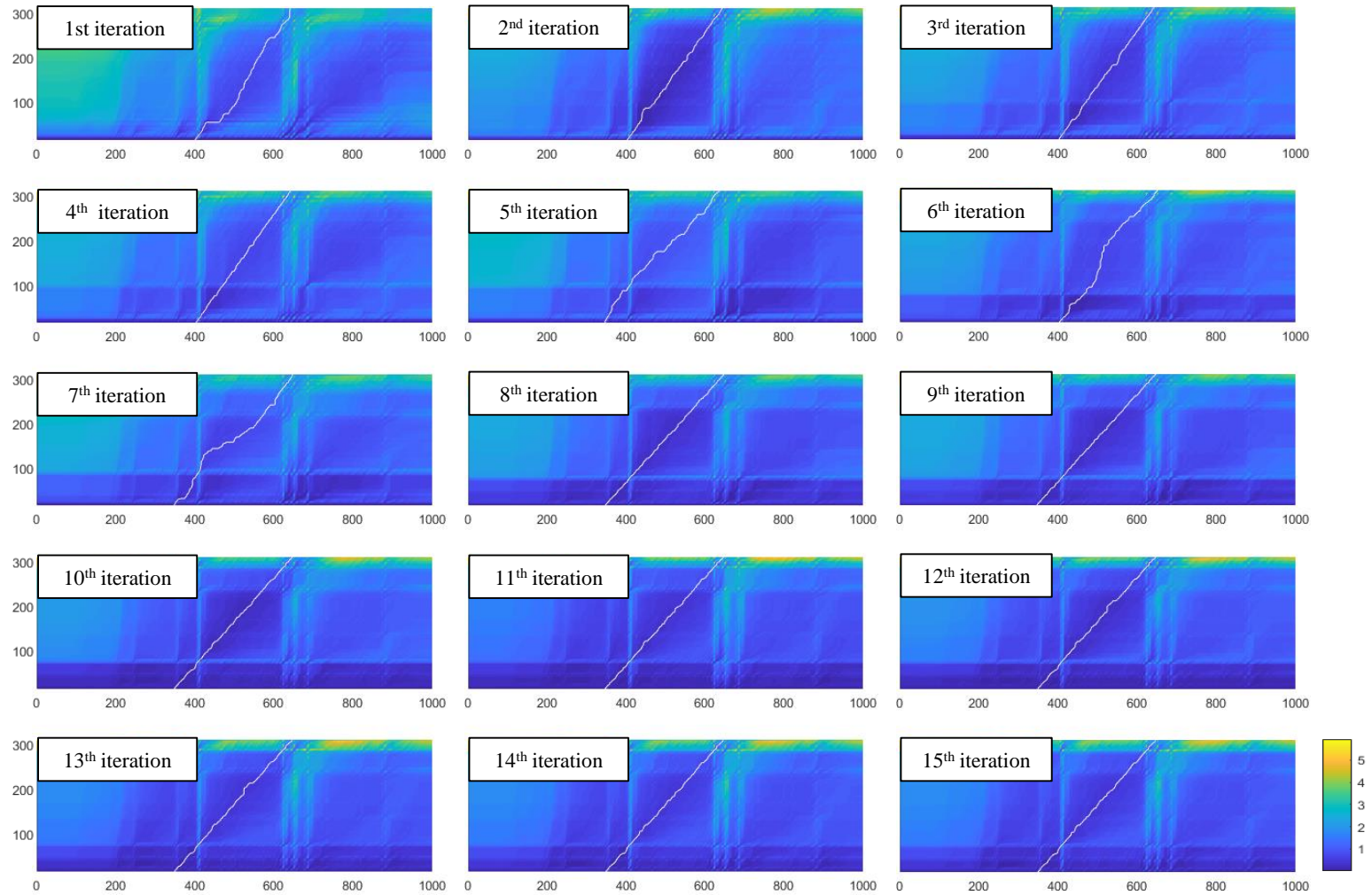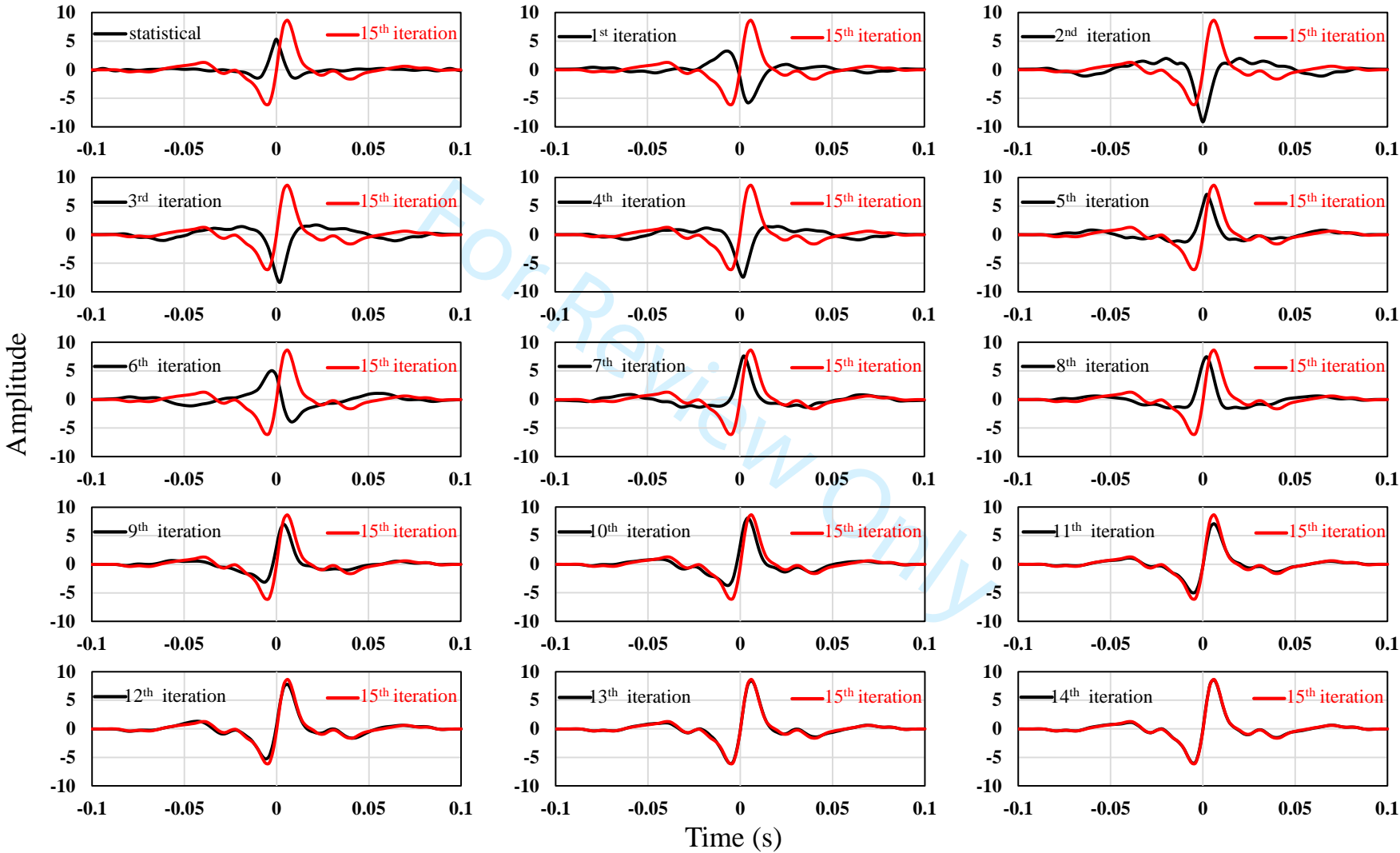
Figure 12
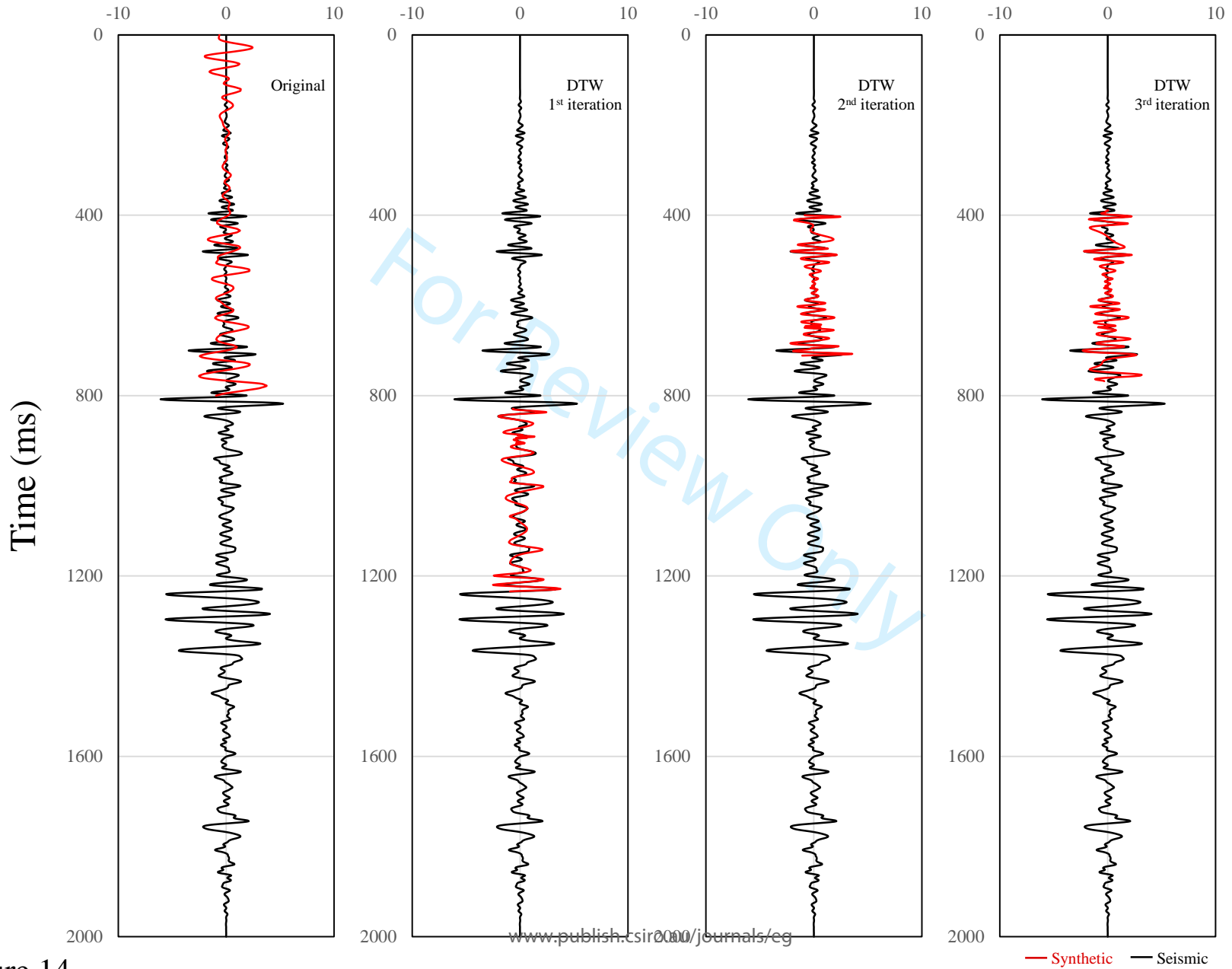
Figure 13

Figure 14
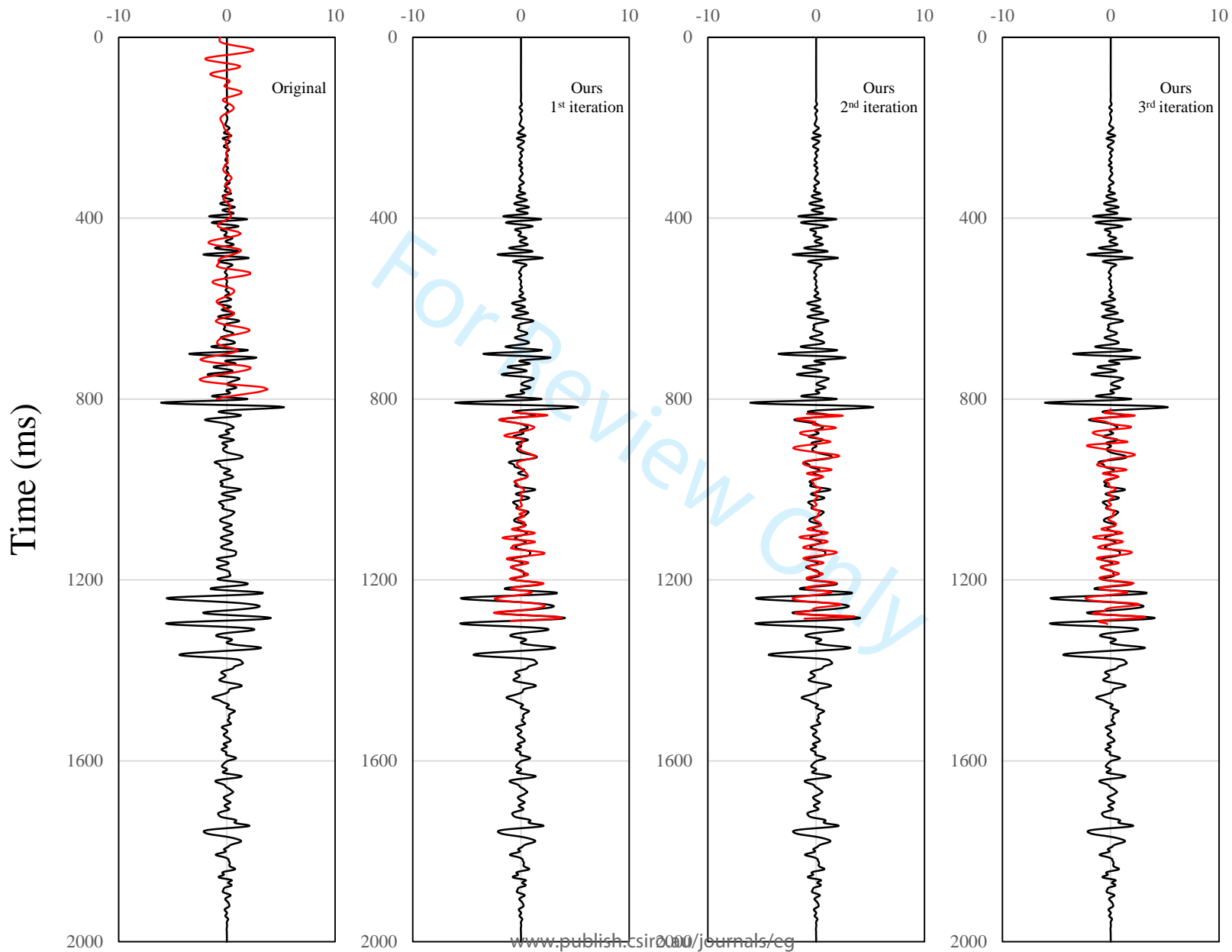
Figure 15

The determination of the constant phase of ~~S~~seismic wavelet ~~phase estimation~~ ~~through~~ ~~automatic~~using automatic ~~seismic~~ seismic-well t~~ying~~ie

Hao Wu[1], Bo Zhang[1], and Danping Cao[2]

[1]The University of Alabama, Department of Geological Science

[2]China University of Petroleum (East China), School of Geoscience

hwu43@crimson.ua.edu, bzhang33@ua.edu, and caodp@upc.edu.cn

Corresponding author:

Bo Zhang

The University of Alabama, Department of Geological Science

bzhang33@ua.edu

ABSTRACT

Seismic wavelet estimation is the bed rock for the ~~seismic well tie~~seismic-well tying and seismic inversion ~~and is a time consuming~~but remain a challenging task. Huge efforts have spent on seismic wavelet estimation and ~~the determination of~~determiningamplitude and phase spectrum ~~is a time consuming task.~~, ~~and most of them focus on the amplitude spectrum estimation and ignore the phase determination.~~ In this paper, we develop a workflow to ~~automatically~~ determine the constant phase of estimated wavelet automatically. Our workflow begins with statistical wavelet estimation and seismic -well tie. We then extract a new seismic wavelet with constant phase by using the well and seismic data together. To obtain the best phase for the extracted wavelet using well and seismic data, we rotate the phase of the wavelet according to a user-defined increment and perform ~~the~~ automatic seismic-well tying for each ~~phase~~ phase-rotated wavelet. The phase, which ~~reaches~~has the maximum correlation coefficient between synthetic and seismic data, is regarded as the best phase for wavelets in each iteration. We next update the time-depth relation according to the result of best seismic -well tie (the maximum correlation coefficient). We repeat the wavelet estimation using well and seismic data, phase rotation, automatic seismic well tie, and time-depth updating procedures until the difference of wavelets, and time-depth relationships in the current and previous iteration is smaller than a user-defined threshold.

Keyword: **Seismic well tie**, **Wavelet**, **Phase**, **DTW**

INTRODUCTION

Seismic wavelet estimation is one of the key procedures for seismic interpretation and inversion. The determination of seismic a wavelet includes amplitude and phase spectrum estimation. Wavelet estimation methods can be classifiedclassify into three main categories: (1) directly deterministic measuring the wavelet, (2) statistically extracting the wavelet from the seismic data and (3) extracting the wavelet by using well-log and seismic data. The deterministic methods require that a seismic-well tie already exists, while the statistical method extracts an average wavelet from a specified window of 3D seismic data (Edgar and van der Baan, 2011). The wavelets Wavelet estimation using well and seismic data incorporates the "prior" reflectivity information in the wavelet estimation (Richard et al., 1988). Statistical wavelets can be estimated from only the seismic data directly without appealing to well logs. Most of the statistical wavelets estimations are based on the assumption that the seismic traces are the a convolution results betweenof the earth's reflectivity and a temporally and spatially invariant zero or minimum phase wavelets. Statistical wavelets assumes that the autocorrelations of amplitude spectra of the seismic data are approximately equal to the seismic wavelet (Yilmaz, 2001).

The determination of the phase spectrum of a seismic wavelet is as important as the determination of the amplitude spectrum of a seismic wavelet. Van der Baan (2008) illustrated that the phase mismatch might result in incorrect horizon picking or seismic well tying. Seismic wavelet phase determination is important for structure and stratigraphic interpretation. Nyman et al. (1987) pointed out the deficiency of zero- and minimum-phase wavelets in the seismic interpretation. Phase mismatch might result in incorrect horizon picking or seismic well tie (van der Baan, 2008). Many techniques have been developed to identify the phase seismic wavelet phase spectrum. Compared to the amplitude spectrum estimation of seismic wavelets,

determining the phase spectrum is far more difficult and ~~presents a~~ significant~~ly~~ ~~effect~~ affects ~~on~~ ~~the~~ seismic inversion (Hampson, 2007). Wiggins (1978) estimated the phase of a seismic wavelet through the minimum entropy deconvolution. ~~It~~ This technique does not~~doesn't~~ need to assume the phase characteristics of ~~the~~ a seismic wavelet. White (1988) proposed to estimate the phase of a seismic wavelet by integrating the maximum kurtosis theory. The advantage of White's method is that there is no requirement for a Gaussian distribution of the subsurface reflectivity series. Levy and Oldenburg (1987) present a method that uses the varimax norm to estimate the residual phase directly; it can make the phase correction automatically. Van der Baan (2008) developed a method, which is based on the maximum kurtosis estimation to obtain ~~the~~ time-varying wavelets. It is robust enough to detect time-varying phase change.

Hampson (2007) pointed out that a constant phase wavelet estimation using well is the most robust method. The estimation of amplitude and phase spectrum of wavelet using seismic does not consider the "prior" reflectivity information contained in the well logs (Richard et al., 1988). There are two main steps for the wavelets estimation using seismic and well data. The first step includes amplitude spectrum estimation using seismic data and reflectivity computed using well logs. The second step is to obtain the optimum phase of the wavelet through seismic-well tying. Nyman (1987) proposed an interactive methodology for the estimation of a seismic wavelet using well control. Their method separately estimated the wavelet's amplitude and phase spectrum. The amplitude spectrum estimation is simply averaging of the ratio between seismic traces spectrum and reflectivity spectrum. Nyman (1987) assumed a constant phase spectrum, and ~~it~~ obtained it through phase and time shift~~ing~~ which maximize~~d~~ the correlation with the synthetic and seismic traces. To obtain the optimal phase for wavelet and time shift for seismic well tie, we usually need more than 10 times manual the seismic well tie and phase scanning of

the seismic wavelet, ~~To obtain the optimal phase and time shift, we usually need more than ten times trail,~~ which is ~~and it is time~~therefore time-consuming. Richard et al. (1988) estimated a linear phase wavelet using well-control. ~~However, Hampson (2007) pointed out that a constant phase wavelet estimation using well is the most robust method. Buland and Omre (2003) proposed to estimate the wavelet from seismic and well data using a Bayesian theory. There are two main steps for the wavelets estimation using seismic and well data. The first step includes amplitude spectrum estimation using seismic data and reflectivity computed using well logs. The second step is to obtain the optimum phase of the wavelet through manually rotate the wavelet phase and seismic well tie. We repeat steps one and until the changing of wavelets is smaller than a user-defined threshold. Usually, we need several hours or even days labor to obtain the optimum wavelets for seismic well ties and inversion.~~

In this paper, we propose a workflow to expedite the estimation of constant phase of seismic wavelet in the seismic well tying. Our workflow is similar with the workflow that proposed by Hampson (2007). However, our workflow can heavily expedite the process of phase determination. We substitute the process of manually optimum phase determination using an automatic procedure. ~~and seismic well tie using wells and seismic data.~~ We ~~realize~~first perform the scanning of phase rotation of the wavelet according to the user-defined range and increment step. We then automatically obtain the corresponding time shift, synthetic squeezing and stretching for each candidate phase by using dynamic time warping (DTW) (Sakoe and Chiba, 1978). The phase ~~which has~~that yields the largest correlation coefficient between seismic and synthetic is ~~regarded~~considered as the best phase in the current loop of seismic well tie. We ~~then~~next estimate the amplitude spectrum of a wavelet ~~by~~using the new time-depth relationship. We next scan the phase and automatically perform the seismic -well tie for each phase rotated

wavelets. We repeat the procedure of amplitude spectrum estimation using well-log data, phase scanning, and automatically seismic-well tie until ~~the changes of seismic wavelets and time-depth relationship in the current and previous iteration are smaller than user-defined thresholds.~~we converge a solution.

METHODOLOGY

A stacked seismic trace can be regarded as the convolution of the seismic wavelet with reflectivity series and added noise:

$$x = r * w + n \tag{1}$$

where x is the seismic trace, r is the reflectivity series, w is the wavelet, n is the noise, and * denote the convolution operator. A wavelet usually is considered a transient signal. It has a start time and an end time, and its energy is confined between these two-time positions (Yilmaz, 2001).

The seismic well tie is the procedure of matching the synthetic seismogram computed using well logs and wavelet to a real seismic trace nearby the borehole place (Walden and White, 1984). We compute the reflectivity series from ~~the~~ a velocity log, $v(z)$, and a density log, $\rho(z)$. The synthetic seismogram is generated by convolving the reflectivity series with a user defined wavelet or a wavelet estimated from the seismic trace ~~a proper wavelet~~. In this paper, we employ ~~the~~ DTW to perform the seismic-well tie through automatically time shifting, stretching and squeezing the synthetic seismogram. DTW is an algorithm for measuring the similarity between two signals (Muller, 2007). The objective of this algorithm is to make an alignment of the two signals through time shifting, squeezing, and stretching one of the signal.

~~Munoz's and Hale (2012, 2015) are the first authors to~~ Several ~~reserchers~~researchers (Munoz and Hale, 2012. Roberto et al, 2012) have proposed ~~a method to employ~~to use DTW ~~in~~

for automatic seismic well tie. Roberto et al (2014) adds a global distance constraint to DTW to prevent the nonphysical alignment. Wu and Gaumon (2017) employed DTW to perform multiple seismic well tie on the flattened syntethic and seismic traces. Error function computation is the first step for DTW to align two signal. We first apply 10 times finer sampling for the synthetic and real seismic traces. The finer interpolation of synthetic and real seismic traces realizes the similar smaller time shift strain of synthetics proposed by Hale(2013). In our seismic well tie, weWe then use the Euclidean distance between synthetic $\mathbf{X} = (x_1, x_2, ..., x_N)$ and real seismic

trace $\mathbf{Y} = (y_1, y_2, ..., y_M)$ $\mathbf{Y} = (y_1, y_2, ..., y_M)$ and real seismic trace $\mathbf{X} = (x_1, x_2, ..., x_N)$ compute

the error matrix $d(i, j)$

$$d(i, j) = \sqrt{(x_i - y_j)^2} , \tag{2}$$

where i, j is the sample index of the refined seismic and synthetic trace, respectively. The total number samples number of the seismic and synthetic traces are M and N, respectively. The second step is to step wisely compute the accumulated error matrix $D(i, j)$ using the error matrix.

$$D(i, j) = d(i, j) + \min\{D(i-1, j-1), D(i-1, j) + d(i-2, j-1), D(i, j-1) + d(i-1, j-2)\} . \tag{3}$$

The final step of DTW is backtracking the minimum cost path within the accumulated error matrix

$$p_L = \arg\min\{D(M, 1) \quad \ldots \quad D(M, N)\} \tag{4a}$$

$$p_{l-1} = \arg\min\{D(i-1, j-1), D(i-1, j) + D(i-2, j-1), D(i, j-1) + D(i-1, j-2)\} , \tag{4b}$$

where L is the total sample number of the backtracked path. We apply the algorithm of dynamic programming to backtrack the path of minimum accumulate Euclidean distance to obtain a

sequence of corresponding index pairs $p = (i,j)$. ~~Note that L is determined by the start point on the accumulated error matrix and it varies with case-by-case. The tracked minimum cost path has the minimum accumulate error. Each point p_{l-1} on the path corresponds to a sample index pair set (i,j)~~ which is the best match~~ing~~ between the synthetic and real traces.

Finally, we can shift, stretch~~ing~~, and squeez~~eing~~ the synthetic to tie it to the real seismic trace according to the tracked minimum cost path. Unfortunately, the occurrence of nonphysical alignment is unavoidable. ~~DTW only can find the minimum cost path and does not consider the shape of the tracked path.~~ In other words, DTW does not consider the shifting, stretching, and squeezing amount for near-by sample of a signal when aligned with another signal. Figure 1a illustrates an example of seismic (black curve) well (red curve) tie using DTW. The red arrows indicate the locations where we need severe stretching of the synthetic trace to tie the seismic trace. The black arrow indicates the location where we need severe squeezing of synthetic trace to tie to the seismic trace. Several methods have been proposed to address this problem. Roberto et al (2012) add a global constraint to the DTW to limit the maximum amount of permitted stretching and squeezing. Hale (2013) refine the error matrix to apply smaller shift strain and achieve smoother path ~~Hale (2013) apply a smoothing constraint to limit the bounds of shift strain. To~~slope. To avoid the severe stretching and squeezing in the real world of seismic well tie, we add a weight term to the accumulated error matrix

$$w_{l1} = \lambda \frac{(t_{l+1} - t_l) - (t_l - t_{l-1})}{(\tau_{l+1} - \tau_l) - (\tau_l - \tau_{l-1})} = \lambda \frac{1 - (t_l - t_{l-1})}{1 - (\tau_l - \tau_{l-1})}$$
$$w_{l2} = \lambda \frac{(t_{l+1} - t_l) - (t_l - t_{l-1})}{(\tau_{l+1} - \tau_l) - (\tau_l - \tau_{l-1})} = \lambda \frac{1 - (t_l - t_{l-1})}{2 - (\tau_l - \tau_{l-1})} \qquad (5a)$$
$$w_{l3} = \lambda \frac{(t_{l+1} - t_l) - (t_l - t_{l-1})}{(\tau_{l+1} - \tau_l) - (\tau_l - \tau_{l-1})} = \lambda \frac{2 - (t_l - t_{l-1})}{1 - (\tau_l - \tau_{l-1})}$$

$$p_l = argmin[D(i-1,j-1) + w_{l1}, D(i-1,j) + D(i-2,j-1) + w_{l2}, D(i,j-1) + D(i-1,j-2) + w_{l3}] \qquad (5b)$$

where the λ denotes the user defined weight, (t_l, τ_l) denote the position index of the optimal matching path. Our proposed weight terms are the second~~ary~~ derivative of the unwrapped path. We are expected to avoid the abrupt change of unwrapped path by minimizing our weighted term. The abrupt change of the path corresponds to sever stretching or squeezing of the synthetic in the seismic well tying, which can limit the variation of path slope between last step and current step. The white curve in Figure 1b shows the tracked optimum cost path using equation 5. We successfully avoid the severe stretching and squeezing shown in Figure 1a. Figures 2a and 2b shows the seismic well tie using the unweighted and weighted backtracking methods, respectively. The cross-correlation coefficients in Figure 2a and 2b are 0.652 and 0.801, respectively.

Figure 3 shows the proposed workflow used to determine the phase of wavelet using the improved DTW. We obtain the amplitude spectrum of proper wavelet using and seismic data and the constant phase by comparing the automatic seismic-well tie for each candidate phase. The workflow is an iterative procedure. It begins with an automatic seismic well tie by DTW. The reflectivity is computed from the well log, and the initial wavelet is the statistical wavelet that is computed from the whole seismic trace. The next step is to extract~~ing~~ the wavelet using well and seismic data (Hampson, 2007). We then rotate the phase of the input wavelet and convolve with the reflectivity to compute a set of synthetic seismogram. We next apply DTW to make an alignment between seismic trace and synthetic seismograms and calculate the correlation between the synthetic and seismic trace. We choose the phase which has the maximum correlation coefficients as the best phase and update the time-depth relationship of the well log. We repeat the steps of extracting wavelet using well and seismic data, phase rotation and seismic well tie, phase selecting and   time-depth relationship updating until and the wavelets and time-

depth relationships in current and previous iteration are smaller than a user-defined threshold (equation 6).

$$\frac{\sum_i \left| W^{(k+1)}(f_i) - W^{(k)}(f_i) \right|}{\sum_i W^{(k)}(f_i)} < 0.001 \tag{6a}$$

$$\left| \varphi^{(k+1)} - \varphi^{(k)} \right| < 2 \tag{6b}$$

$$\frac{\sum \left| T^{(k+1)}(j) - T^{(k)}(j) \right|}{N} < 0.001 \tag{6c}$$

where $W^{(k)}(f_i)$ is the amplitude spectrum of the wavelet in the kth iteration of seismic well tie, φ is the constant phase of the wavelet, $T_k(i)$ is the time shift for the jth sample of the synthetic, and N is the total sample number of the synthetic.

APPLICATION

Real data example

To demonstrate the effectiveness of our workflow, we apply it to a seismic survey acquired over the Fort Worth Basin. We use one well within the seismic survey to demonstrate the proposed workflow. Figure 4 shows the extracted 200 ms statistical wavelet from the poststack seismic using the Hampson-Russell commercial software. The extracted statistical wavelet is used as the initial wavelet for the seismic well tie using DTW. The first, second, third, and fourth panels in Figure 5 are the density, P-wave velocity, computed reflectivity, and computed synthetic, respectively. We compute the synthetic through the convolution between the reflectivity shown in the third panel of Figure 5 and wavelet shown in Figure 4. Figure 6a shows the synthetic (red curve) overlaid on the real seismic trace at the wellbore location before automatic seismic well tie. The horizontal axis is the sample index of the two sequences

(synthetic and real seismic trace). In our case, we only have p-wave and density logs within a limited depth zone. The length of the synthetic is much smaller than that of the seismic traces. Figure 6b shows the results of automatic seismic-well tie using the statistical wavelet.

We begin our phase determination after we obtain a rough seismic well tie shown in Figure 6b. We iteratively extract the wavelet using well and seismic data with constant phase. Figure 7 shows the extracted wavelet using well and seismic data in the first iteration. The initial phase of the exacted wavelet shown in Figure 8 is 129°. We then rotate the phase of the wavelet and convolve the phase rotated wavelet with the reflectivity to generate the synthetic seismogram. In this paper, we rotated the phase from 0° to 359° with a step of 1°. Figure 8 shows six representative phase rotated wavelets with rotation amount of 0, 60°, 120°, 180°, 240°, 300°. The phase of the rotated wavelets shown in Figure 8 are 129°, 189°, 249°, 309°, 9°, 69°, respectively. We next apply DTW to perform the automatic seismic well tie between the synthetic and the seismic trace and compute the correlation coefficient for each seismic well tie. Figure 9 shows six representative results of automatic seismic well ties in the first iteration for the 0, 60°, 120°, 180°, 240°, 300° phase rotated wavelets. We perform 360 times automatically perform seismic well ties 360 times in each iteration and roughly need 30 seconds in for each iteration. Figure 10 shows the cross-correlation coefficient varying with phases of wavelets. We obtain the cross-correlation coefficients in Figure 10 by comparing the similarity between synthetic and seismic trace after the seismic well tie. According to the cross-correlation coefficients shown in Figure 10, the best phase for the wavelet in the first iteration is 125°. The last processing in each iteration is updating the time-depth relationship according to the seismic well tie with the maximum correlation coefficient.

There ~~is~~ are ~~a~~ negligible changes for both wavelets and seismic well ties after 15 ~~times~~ iterations in our case. Figure 11 shows the seismic well tie for each iteration. The red and black curve are the synthetic and seismic traces, respectively. Note the changes of the seismic well tie is negligible starting from 8th iteration. Figure 12 shows the accumulated error matrix and optimal warping minimum cost path (white curve). Figure 13 shows wavelets changing with the iteration number of seismic well tie. The black and red curve are the wavelet with best phase in each iteration and the final optimum wavelet, respectively. Note that there ~~is a~~are negligible changes for the shape and phase of the seismic wavelet after 15 times iteration. We obtain our best wavelet after 15 times in our application according to the criteria defined in Equation 6.

Comparison with conventional DTW

To illustrate the robustness of our proposed workflow, we also compare our method with the conventional DTW. We selected the same seismic data and well log data from the Fort Worth Basin. We iteratively apply DTW and our method to align the synthetic seismogram from the well log with the real seismic trace. The black and red curves in the first panel of Figure 14-15 are the real seismic trace and original synthetic seismogram, respectively. The black and red curves in the second, third and fourth panel of Figure 14-15 are the 1st to 3rd iteration result of real seismic trace and tied synthetic seismogram by DTW and our method, respectively. In figure 14, the synthetic seismogram shows some abrupt velocity changing part and based on the well top data, the synthetic tied to the wrong position of the seismic trace. Noted that in Figure 15, using our method get higher cross-correlation, the synthetic has tied to the right position of seismic trace and the change of time-depth relationship has meet the defined threshold.

Formatted: Indent: First line: 0"

CONCLUSIONS

We present a novel workflow to estimate the wavelet phase automatically. In this paper, we first improve the DTW algorithm by adding a second derivative weight in the error matrix computation. The weighted term is designed for avoid the severe stretching or squeezing of synthetic in the process of seismic well ties. We then obtain the best phase of a wavelet by performing iteratively automatic seismic well tie using our proposed modified DTW algorithm. The application and comparison illustrate that our workflow not only obtains the best phase of wavelet for the seismic well but also improves the quality of the seismic well tie. Moreover, our workflow also heavily expedite the process of wavelet phase estimation and seismic well tie when compared to the manual seismic well tie.

In this paper, we first improve the DTW algorithm in seismic well tie to avoid the severe stretching or squeezing of synthetic. We then develop a new workflow to automatically determine the best phase of wavelet used for seismic well tie. Our workflow not only obtains the best phase of wavelet for the seismic well but also improves the quality of the seismic well tie. In our application, the time cost of the automatic seismic well tie in each iteration is around 10 seconds. The time cost of our whole workflow is around 5 minutes which include the wavelet estimation and time depth relationship updating. By contrast, we need more than 10 minutes for manual phase scanning of wavelets in one iteration using the commercial software. Thus our workflow can heavily expedite the procedure of seismic well tie.

LIST OF FIGURE CAPTIONS

Figure 1. Cartoon illustrating seismic well result using original and imprvoed DTW aglorihtms. (a) The accumulated error matrix and optimal warping path using original DWT. (b) The accumulated error matrix and optimal warping path using improved DTW.

Figure 2. The seismic well tie results using (a) DTW and (b) improved DTW. The improved DTW successfully avoids the severe stretching and squeezing.

Figure 3. The proposed workflow of the seismic phase determination.

Figure 4. The initial extracted statistical wavelet using commercial software.

Figure 5. The well logs and synthetic used for seismic well tie. The first, second, third, and fourth panel are the density log, velocity log, computed reflectivity and computed synthetic seismogram, respectively.

Figure 6. The synthetic (red) and seismic (black) (a) before and (b) after seismic well tie.

Figure 7. The extracted wavelet using well and seismic data in the first iteration.

Figure 8. The six representative phase rotated wavelets in the first iteration of seismic well tie. The initial phase of the wavelet is 129°. The phases of the phase rotated wavelets are 129°, 189°, 249°, 309°, 9°, and 69°.

Figure 9. The six representative results of automatic seismic well tie in the first iteration for the 0, 60°, 120°, 180°, 0°, and 300o phase rotated wavelets.

Figure 10. The cross-correlation coefficient between seismic well tie for the phase rotated wavelets the first iteration.

Figure 11. The seismic well tie results in each iteration.

Figure 12. The accumulated error matrix overlaid with the optimum minimum cost path (white curve) in each iteration.

Figure 13. The wavelets with the best phases in each iteration. The black and red curves are the wavelet with the best phase and the final best wavelets, respectively.

Figure 14. The test of DTW in real data. The first panel shows the original synthetic seismogram (red) overlaid on the seismic trace (black), the second to fourth panels shows the 1st to 3rd iteration results of seismic trace (black) and tied synthetic seismogram (red). The tied synthetic seismogram are tied to the wrong position and shows some abrupt changing of time-depth relationship.

Figure 15. Illustrating that our proposed method applied on the real seismic data. The first panel shows the original synthetic seismogram (red) overlaid on the seismic trace (black), the second to fourth panels shows the 1st to 3rd iteration results of seismic trace (black) and tied synthetic seismogram (red). Noted that the tied synthetic seismogram meet the defined threshold and get an excellent seismic well tie after three times iteration.

REFERENCE

Buland, A., and H. More, 2003, Jonint AVO inversion, wavelet estimation and noise-level estimation using a spatially coupled hierarchical Bayesian model, Geophysical Prospecting, **51**, 531-550.

Edgar, J., and M. van der Baan, 2011, How reliable is statistical wavelet estimation?: Geophysics, **76**, no. 4, V59–V68.

Hampson, D., 2007, Theory of the Strata program: Technical report, CGG Hampson-Russell.

Hale, D., 2013, Dynamic warping of seismic images: Geophysics, 78, no. 2, S105–S115.

Herrera, R., H., and M., van der Baan, 2012, Guided seismic-to-well tying based on dynamic time warping, SEG Expanded Abstracts

Herrera, R. H., S. Fomel, and M. van der Baan, 2014, Automatic approaches for seismic to well tying: Interpretation, **2**, no. 2, SD101–SD109

Levy, S., and D. W. Oldenburg, 1987, Automatic phase correction of common-midpoint stacked data: Geophysics, **52**, 51-59.

Liner, C. L., 2002, Phase, phase, phase: The Leading Edge, **21**, 456-457.

Longbottom, J., A. T. Walden, and R.E. White, 1988, Principles and application of maximum kurtosis phase estimation: Geophysical Prospecting, **36**, 115-138.

Mueller, M., 2007, Dynamic time warping in information retrieval for music and motion: Springer.

Muñoz, A., and D. Hale, 2012, Automatically tying well logs to seismic data, CWP-725.

Muñoz, A., and D. Hale, 2015, Automatic simultaneous multiple well ties: Geophysics, **80**, no. 5, IM45–IM51.

Nyman, D. C., M. J. Parry, and R. D. Knight, 1987, Seismic wavelet estimation using well control, SEG Expanded Abstracts, 211-213.

Richard, V., and J. Brac, 1988, Wavelet analysis using well log information. SEG Expanded Abstracts, 946-949.Robinson, E. A., 1957, Predictive decomposition of seismic traces: Geophysics, **22**,767-778.

Robinson, E. A., and S. Treitel, 1967, Principles of digital Wiener filtering: Geophysical Prospecting, **15**, 311-332.

Sakoe, H., and S. Chiba, 1978, Dynamic programming algorithm optimization for spoken word recognition: IEEE Transactions on Acoustics, Speech, and Signal Processing, **26**, 43-49.

Stone, D. G., 1984, Wavelet estimation: Proc. IEEE, **72**, 1394-1402.

van der Baan, M., 2008, Time-varying wavelet estimation and deconvolution by kurtosis maximization: Geophysics, **73**, no.2, V11-V18.

van der Baan, M., and S. Fomel, 2009, Nonstationary phase estimation using regularized local kurtosis maximization: Geophysics, 74, A75-A80.

van der Baan, M., S. Fomel, and M. Perz, 2010, Nonstationary phase estimation: A tool for seismic interpretation?: The Leading Edge, **29**, 1020-1026.

Walden, A. T., and J. W. J. Hosken, 1985, An investigation of the spectral properties of primary reflection coefficients: Geophysical Prospecting, **33**, 400-435.

Walden, A. T., and R. E. White, 1984, On errors of fit and accuracy in matching synthetic seismograms and seismic traces: Geophysical Prospecting, **32**, 871-891.

White, R. E., 1988, Maximum kurtosis phase correction: Geophysical Journal International, **95**, 371-389.

White, R. E., and P. N. S. O'Brien, 1974, Estimation of the primary seismic pulse: Geophysical Prospecting, **22**, 627-651.

White, R., and T. Hu, 1997, How accurate can a well tie be?: SEG Expanded Abstracts, **16**, 816.

White, R., and R. Simm, 2002, Phase, polarity and the interpreter's wavelet: EAGE first break, **20**, 277-281.

White, R., and R. Simm, 2003, Tutorial: Good practice in well ties: EAGE first break, **21**, 75-83.

Wiggins, R., 1978, Minimum entropy deconvolution: Geoexploration, **16**, 21-35.

Wu, X., and G. Caumon, 2016, Simultaneous multiple well-seismic ties using flattened synthetic and real seismograms: Geophysics, **82**, no. 1, IM13–IM20

Yilmaz, Ö., 2001, Seismic data analysis: processing, inversion, and interpretation of seismic data: Society of Exploration Geophysicists.

Revision Notes

==

Replies to Editor and Reviewers

First of all, we thank both the Editor J. Chen and the reviewers for their thorough and valuable review, as well as constructive comments and fruitful suggestions, which have contributed in improving the quality of the paper.

==

Reply to the Editor

Dear Editor J. Chen,

We appreciate for your valuable suggestions and encouragement. During the past weeks, we have tried our best to improve the quality of this manuscript following the reviewers' explicit guides. Specifically, we have made an effort to improve the grammar, and the fragment sentences have been explained and rewritten carefully in the revised manuscript. At the same time, the point-by-point responses to the comments are given below. We hope to publish the best paper in the Exploration Geophysics to share our idea.

Thank you for all your time and energy regarding our manuscript. We are looking forward to hearing from you soon.

Yours Sincerely

Hao Wu

Dear Reviewer,

We are grateful to your constructive comments and fruitful suggestions, which we believe enhance the paper after incorporating them into the manuscript. In the past a few weeks, we have tried our best to improve the quality of this manuscript and to make it acceptable.

In the revised manuscript, we have compared our work with some other example of applying dynamic time warping for seismic well tying and highlight my contribution based on the comparison. The fragment sentences in the manuscript have been explained and rewritten carefully to make them much clearer. We have tried our best to make the revised manuscript much more complete and valuable. Thank you once again for your great suggestions and corrections.

Best regards,

Hao Wu

Comments and Responses

Comments 1

Can you explain why the formulation is different from the original algorithm?

Response: The original DTW algorithm only consider the minimum accumulation path between the original sequence and reference sequence and did not consider the relative shifting amount of nearby samples. We will have sever stretching or squeezing if there is a large shifting difference between nearby samples. In our proposed method, we add a weighted term in the objective

function for seismic well tie to avoid abrupt velocity change. As a result, our method can avoid severe squeeze and stretch.

Comments 2

Also, the formulation only allows for time shifts and strain in one direction, is there a reason for this?

Response: Our formulation allows for time shifts and strain in both direction. The direction of the time shift can be represented by the slope of the path. The direction of the time shift is positive if the slope of the path is smaller than 45 degree. As a result, we stretch the reference sequence. The direction of the time shift is negative if the slope is larger than 45 degree. As a result, we squeeze the reference sequence.

Comments 3

"To obtain the optimal phase and time shift, we usually need more than ten time trail." What does this mean?

Response: We have revise this sentence as follows:

"To obtain the optimal phase for wavelet and time shift for seismic well tie, we usually need more than 10 times manual the seismic well tie and phase scanning of the seismic wavelet."

Comments 4

"The synthetic seismogram is generated by convolving the reflectivity series with a proper wavelet." What is a "proper" wavelet?

Response: Many thanks for your valuable question. We have revised the "proper" to "a user defined wavelet or a wavelet estimated from the seismic trace."

Comments 5

"we use the Euclidean distance between synthetic $\mathbf{Y} = (y_1, y_2, ..., y_M)$ and real seismic trace $\mathbf{X} = (x_1, x_2, ..., x_N)$ compute the error matrix $d(i,j)$." This shows vectorized form of X and Y, which do not match the formula below. I would request consistent annotation.

Response: Many thanks for your great suggestion. I have revised the X and Y to synthetic $\mathbf{X} = (x_1, x_2, ..., x_N)$ and real seismic trace $\mathbf{Y} = (y_1, y_2, ..., y_M)$

Comments 6

$$D(i,j) = d(i,j) +$$
$$\min\{D(i-1,j-1), D(i-1,j) + d(i-2,j-1), D(i,j-1) + d(i-1,j-2)\}$$

$$p_{l-1} = \arg\min\{D(i-1,j-1), D(i-1,j) + D(i-2,j-1), D(i,j-1) + D(i-1,j-2)\}$$

Draw this out. Also, this formula will only allow time shifts and strain in one direction. Go back and look at the original formulation in Sakoe and Chiba, Muller, or Hale. You can vary this formulation for additional constraints on strain, which increases computational cost. If there is a specific reason this formula is different from the original algorithm, you should explain why.

Response: We have double checked that the above equations are the same with the equations shown in the paper of Munoz and Hale (2012). The only difference is the notation. We employ d standing for the error matrix. Munoz and Hale employed e standing for the error matrix.

Comments 7

"Note that L is determined by the start point on the accumulated error matrix and it varies with case-by-case. The tracked minimum cost path has the minimum accumulate error. Each point p_{l-1} on the path corresponds to a sample index pair set (i, j) which is the best matching between the synthetic and real traces." This explanation is hard to follow.

Response: Many thanks for your great suggestion. We have revised those sentences to "We apply dynamic wrapping to backtrack the path of minimum accumulate Euclidean distance between the two sequences. The point of the path is denoted as p_l , where l is index of the path. We have a series of index pair (i, j) corresponding to each of points on the path, where i and j are the index of the two sequences."

Comments 8

$$w_{l1} = \lambda \frac{(t_{l+1} - t_l) - (t_l - t_{l-1})}{(\tau_{l+1} - \tau_l) - (\tau_l - \tau_{l-1})} = \lambda \frac{1 - (t_l - t_{l-1})}{1 - (\tau_l - \tau_{l-1})}$$

$$w_{l2} = \lambda \frac{(t_{l+1} - t_l) - (t_l - t_{l-1})}{(\tau_{l+1} - \tau_l) - (\tau_l - \tau_{l-1})} = \lambda \frac{1 - (t_l - t_{l-1})}{2 - (\tau_l - \tau_{l-1})}$$

$$w_{l3} = \lambda \frac{(t_{l+1} - t_l) - (t_l - t_{l-1})}{(\tau_{l+1} - \tau_l) - (\tau_l - \tau_{l-1})} = \lambda \frac{2 - (t_l - t_{l-1})}{1 - (\tau_l - \tau_{l-1})}$$

Please define the lambda, tau and t.

Response: Many thanks for your valuable suggestion. We have added a definition "where the λ denotes the user defined weight, (t_l, τ_l) denote the position index of the optimal matching path."

Comments 9

$$p_k = \mathrm{argmin}[D(i-1, j-1) + w_{l1}, D(i-1, j) + D(i-2, j-1) + w_{l2}, D(i, j-1) + D(i-1, j-2) + w_{l3}]$$

Refer to my previous comments about the formulation of this term.

Response: Our formation allow time shifts and strain in both direction. We also consider the relative shifting amount of nearby samples of the sequence when backtrack the optimal matching path.

<u>Comments 10</u>

"In this paper, we first improve the DTW algorithm in seismic well tie to avoid the severe stretching or squeezing of synthetic." Give a quick restatement about what you do differently with your distance weights.

Response: Many thanks for your valuable suggestion. We have revised our conclusion as follows: "We present a novel workflow to estimate the wavelet phase automatically. In this paper, we first improve the DTW algorithm by adding a second derivative weight in seismic well tie to avoid the severe stretching or squeezing of synthetic. We then employ the modified DTW algorithm to develop a new workflow to automatically determine the best phase of wavelet used for seismic-well tie. The application and comparison illustrate that our workflow not only obtains the best phase of wavelet for the seismic well but also improves the quality of the seismic well tie. Moreover, our workflow also heavily expedite the process of wavelet phase estimation and seismic well tie, which can save a lot of labor work."

<mark>Reply to the Reviewer 2</mark>

Dear Reviewer,

We are grateful to your constructive comments and fruitful suggestions, which we believe enhance the paper after incorporating them into the manuscript. In the past a few weeks, we have tried our best to improve the quality of this manuscript and to make it acceptable.

In the revised manuscript, we have compared our work with some other example of applying dynamic time warping for seismic well tying and highlight my contribution based on the comparison. The fragment sentences in the manuscript have been explained and rewritten carefully to make them much clearer. We have tried our best to make the revised manuscript much more complete and valuable. Thank you once again for your great suggestions and corrections.

Best regards,

Hao Wu

<mark>Comments and Responses</mark>

Comments 1

You claimed "The weight terms in equation 5a are a secondary derivative of unwrapped path. We can avoid the variation of path slope by minimizing the weighted term. The abrupt change of the path corresponds to severe stretching and squeezing of synthetic." in replying to 1st reviewer's questions. However you dodged the question of reviewer 3 regarding how to

incorporate smaller shift strain or path slope constraints to compute more stable optimal path. I find this contradictory, please explain more regarding this issue.

Response: Many thanks for your great efforts and suggestion. Regarding to the question of reviewer 3, in Hale's DTW method (Hale, 2013), the error matrix is defined by the following equation:

$$e[i,l] = (f[i] - g[i+l])^2 \qquad (1)$$

where $e[i,l]$ is the error matrix, $f[i]$ and $g[i]$ represent the original sequence and reference sequence, respectively. l denotes the integer time lag and approximately equals to the time shift. The objective of this function is to minimize the error $e[i,l]$ and find out the corresponding time shift l of each point. Moreover, Hale (2013) refine the error matrix that make time shift not need to be integer, but can also be -0.5 or 0.5. This improvement is the method of how to incorporate smaller shift strain that reviewer 3 mentioned.

However, the error matrix in this paper is defined by equation 2 (Sakoe and Chiba, 1978):

$$e[i,j] = (f[i] - g[j])^2 . \qquad (2)$$

We can simply realize the same function defined in equation 1 by finer interpolate both synthetic and real seismic traces prior the seismic well tie. In this paper, we interpolate fine interpolated 10 times before the seismic well time and coarse interpolate 10 times after the seismic well-tie. We minimize the error matrix to find out the matched points index pair $[i,j]$ between the original sequence and reference sequence. So we are not incorporating the method of smaller shift strain that proposed by Hale (2013). We first apply 10 times finer sampling for the synthetic and real

seismic traces. The finer interpolation of synthetic and real seismic traces realizes the similar smaller time shift strain of synthetics proposed by Hale(2013).

Comments 2

Following my previous question, I would suggest you demonstrate comparison of results using your proposed weighting functions with well-established DTW methods. As you mentioned, the proposed weighting terms are one of two major contributions of this work. You need to show some comparison results to demonstrate validity of your work.

Response: Many thanks for your great suggestion. We have revised our paper and add a section about the comparison between the conventional DTW method and our proposed method. Here are the added section and figures.

Comparison with conventional DTW

To illustrate the robustness of our proposed workflow, we also compare our method with the conventional DTW. We selected the same seismic data and well log data from the Fort Worth Basin. We iteratively apply DTW and our method to align the synthetic seismogram from the well log with the real seismic trace. The black and red curves in the first panel of Figure 14-15 are the real seismic trace and original synthetic seismogram, respectively. The black and red curves in the second, third and fourth panel of Figure 14-15 are the 1st to 3rd iteration result of real seismic trace and tied synthetic seismogram by DTW and our method, respectively. In figure 14, the synthetic seismogram shows some abrupt velocity changing part and based on the well top data, the synthetic tied to the wrong position of the seismic trace. Noted that in Figure 15, using our method get higher cross-correlation, the synthetic has tied to the right position of seismic trace and the change of time-depth relationship has meet the defined threshold.

Figure 14
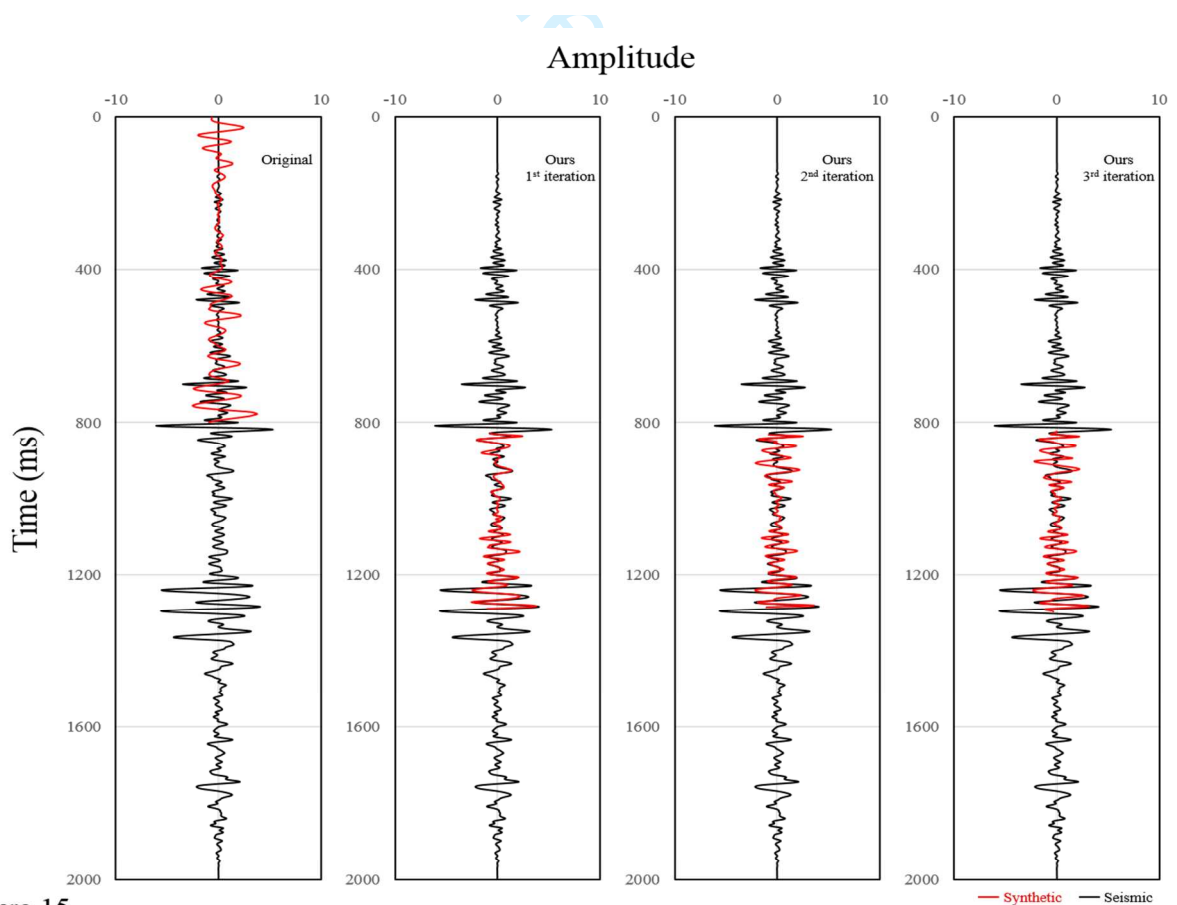
Figure 15

Comments 3

Conclusions in current manuscript t are too vague. Analyze complexity of your algorithm and compare with others if you want to prove efficiency of your algorithm. The term "around 10 seconds" is meaningless. It is also pointless to say your workflow takes about 5 minutes and it might take 10 minutes by using commercial software since there is no details about what circumstance you are discussing about. The Conclusions section needs to be rewritten using proper scientific terms.

   Response: Many thanks for your great suggestion. We have revised our conclusion with following sentences: "We present a novel workflow to estimate the wavelet phase automatically. In this paper, we first improve the DTW algorithm in seismic well tie to avoid the severe stretching or squeezing of synthetic. We then employ the modified DTW algorithm to develop a new workflow to automatically determine the best phase of wavelet used for seismic-well tie. The application and comparison illustrate that our workflow not only obtains the best phase of wavelet for the seismic well but also improves the quality of the seismic well tie. Moreover, our workflow also heavily expedite the process of wavelet phase estimation and seismic well tie, which can save a lot of labor work."

Reply to the Reviewer 3

Dear Reviewer,

We are grateful to your constructive comments and fruitful suggestions, which we believe enhance the paper after incorporating them into the manuscript. In the past a few weeks, we have tried our best to improve the quality of this manuscript and to make it acceptable.

In the revised manuscript, we have compared our work with some other example of applying dynamic time warping for seismic well tying and highlight my contribution based on the comparison. The fragment sentences in the manuscript have been explained and rewritten carefully to make them much clearer. We have tried our best to make the revised manuscript much more complete and valuable. Thank you once again for your great suggestions and corrections.

Best regards,

Hao Wu

Comments and Responses

Comments 1

This manuscript has been significantly improved after the revision. However, I do not think the authors understand my second comment on the shift strains. Firstly, small shift strains does not mean small shifts. Shift strain is the first derivative of shifts, and therefore the shift strain

controls the smoothness or the "shape" of the minimum path. Smaller shift strains will yield smoother paths, and a smooth path could correspond to large correlation shifts.

Response: Many thanks for your great efforts and suggestion. Since we use different equation with Hale's (2013) paper to define the error matrix. In Hale's method, the objective is to find the time shift for each point, and set the shift strain or variation between current point and next point is smaller than 0.5. However, according to the equation of error matrix, the objective of our method is to find the corresponding pairs index between the original sequence and reference sequence. We first apply 10 times finer sampling for the synthetic and real seismic traces. The finer interpolation of synthetic and real seismic traces realizes the similar smaller time shift strain of synthetics proposed by Hale(2013).

Comments 2

Secondly, in Dave's DTW method (Hale, 2013, Dynamic warping of seismic images), no finer interpolation is applied. Moreover, in Dave's DTW paper, no seismic well tying is discussed.

Response: Many thanks for your great suggestion. We have revised our paper with properly reference: "Hale (2013) refine the error matrix to apply smaller shift strain and achieve smoother path slope."